Journal of Water Process Engineering 76 (2025) 108109

Contents lists available at ScienceDirect

Journal of Water Process Engineering

journal homepage: www.elsevier.com/locate/jwpe

Comparative photo electro catalytic oxidation of real pharmaceutical wastewater using Ag/TiO_2: Process optimization and acute toxicity removal

Ayse Elif Ates [a], Sinan Ates [a,*], Serdar Aydın [a], Gamze Varank [b]

[a] Department of Environmental Engineering, Engineering Faculty, Istanbul University-Cerrahpasa, Avcilar, Istanbul, Turkey
[b] Yildiz Technical University, Faculty of Civil Engineering, Department of Environmental Engineering, 34220 Esenler, Istanbul, Türkiye

ARTICLE INFO

Editor: Sadao Araki

Keywords:
Photo electro catalysis
Real pharmaceutical wastewater
Ag/TiO_2
Ecotoxicity
Process optimization

ABSTRACT

Pharmaceutical wastewater contains persistent organic pollutants and bioactive compounds that pose significant environmental risks. Despite extensive studies on photocatalytic degradation, research on real pharmaceutical wastewater remains limited. This study evaluates the performance of silver-doped titanium dioxide (Ag/TiO_2) in real pharmaceutical wastewater treatment through photo electro catalytic oxidation (PECO) and electro catalytic oxidation (ECO), with a focus on process optimization, pollutant removal efficiency, and ecotoxicological impacts, and the comparative performance of Ag/TiO_2 as both anode and cathode materials. A Central Composite Design (CCD) approach was employed to systematically analyze the effects of pH, reaction time, current density, and temperature on chemical oxygen demand (COD) and UV_{254} removal efficiencies. Response Surface Methodology (RSM)-based correlation models accurately predicted Results with 98 % reliability. Under optimized conditions, PECO demonstrated its high efficiency in wastewater treatment by achieving 76 % COD and 86 % UV_{254} removal. Unlike similar studies in literature, which often ignore the synergistic effects of resistant pollutants, this study provides a comprehensive and realistic ecotoxicological assessment. Acute toxicity tests using *Daphnia magna* revealed that untreated wastewater caused 97 % immobilization, while PECO reduced it to 23 % without dilution in 30 min, highlighting its superior detoxification potential.

1. Introduction

The pharmaceutical industry generates complex wastewater containing active pharmaceutical ingredients, intermediates, and solvents because of various processes such as equipment cleaning and extraction [1]. The literature indicates that pharmaceutical compounds exhibit strong correlations with other contaminants in wastewater, highlighting the critical need to assess their synergistic or antagonistic effects [2,3]. However, due to the chemical resistance of pharmaceutical compounds, conventional treatment methods are often insufficient for their removal and fail to provide an effective solution [4]. In this context, hybrid treatment systems that integrate advanced oxidation processes with conventional biological or physicochemical methods hold significant promises for the effective treatment of pharmaceutical wastewater [5]. Among advanced oxidation processes, electro-catalytic oxidation and photo-electro-catalytic oxidation have demonstrated high efficiency in degrading complex pharmaceutical pollutants while mitigating their toxic effects, thus offering a more environmentally sustainable alternative [6,7].

Electrocatalytic oxidation (ECO) has emerged as a promising and effective water treatment technology for the removal of persistent organic pollutants. This process facilitates the degradation of contaminants through the generation of highly reactive oxygen species (ROS), such as hydroxyl radicals (OH•) and superoxide radicals (O_2^{-}•), which are electrochemically produced at the electrode surface [8,9] ECO offers significant advantages, including operational flexibility and high efficiency, particularly in the treatment of complex pollutant mixtures [10]. The overall performance of the ECO process can be further improved by optimizing key operational parameters, such as the selection of electrode materials, electrochemical catalysts, and the applied current density. [8]. However, high energy consumption and electrode degradation present significant challenges to the large-scale implementation of this technology [11]. To overcome these limitations, photo-electrocatalytic oxidation was developed as a hybrid process by integrating it with the photocatalysis process of ECO [12]. This synergistic approach is considered a promising solution to improve treatment efficiency while reducing operational costs [8].

In the photo-electro-catalytic oxidation process, a semiconductor

* Corresponding author.
E-mail addresses: sinanates@ogr.iuc.edu.tr, sinanates89@gmail.com (S. Ates).

https://doi.org/10.1016/j.jwpe.2025.108109
Received 14 April 2025; Received in revised form 23 May 2025; Accepted 4 June 2025
2214-7144/© 2025 Elsevier Ltd. All rights are reserved, including those for text and data mining, AI training, and similar technologies.

catalyst is activated by both light and electrical energy, leading to the generation of OH• and other reactive oxygen species. Solar irradiation induces electron-hole pair formation on the surface of the semiconductor material, while the application of an electric potential to the electrode and catalyst facilitates the separation of these charge carriers, thereby accelerating the reduction or oxidation of pollutants [13]. Compared to conventional oxidation processes, this approach enables the effective removal of a broader range of contaminants [14]. Additionally, since the reaction operates at lower temperatures and under atmospheric pressure, energy consumption is minimized, enhancing the overall economic efficiency of the process [15].

Titanium dioxide (TiO_2) is widely preferred owing to its low cost, abundant availability, excellent chemical stability, and environmentally benign, non-toxic nature. [16]. However, its limited efficiency under visible light suggests the need for modification strategies to improve its performance. [17]. Recent studies have demonstrated that doping TiO_2 with silver (Ag) can significantly improve its photocatalytic activity [18]. The incorporation of Ag into TiO_2 suppresses electron-hole recombination, thereby enhancing charge carrier efficiency, while also extending light absorption into the visible spectrum, which improves photocatalytic performance [19]. Additionally, Ag-doped photocatalysts exhibit strong oxidative effects on pathogens, reducing the reliance on UV light and thus enabling lower energy consumption with higher oxidation efficiency [20]. In this context, Ag-doped TiO_2 offers considerable potential for the development of sustainable and high-efficiency photocatalysts.

Ag-doped TiO_2 photocatalysts have shown promising results in the treatment of pharmaceutical industry wastewater [21]. Due to their strong inhibitory and antibacterial properties, as well as their high efficiency in targeting specific contaminants, Ag NPs are widely used in the treatment of pharmaceutical industry wastewater [22,23]. However, the photocatalytic oxidation process is influenced by various parameters such as temperature, duration, current density, and pH, making the optimization of these factors crucial for achieving maximum removal efficiency [24]. RSM is an effective tool for process optimization and analyzing parameter interactions by modeling the relationships between independent variables and one or more outputs. RSM is widely used to determine optimal operating conditions and simultaneously evaluate multiple responses, while minimizing costs and time by reducing the number of experiments [25,26].

This study evaluated the effectiveness of ECO and PECO processes using TiO_2 and Ag/TiO_2 coated electrodes for the treatment of real pharmaceutical wastewater, highlighting the potential of advanced oxidation processes to deliver realistic and applicable results. Studies in literature focusing on specific pollutants often neglect the possible synergistic or antagonistic interactions between these compounds, which consequently limit their representation in real wastewater matrices [27]. In this study, the removal efficiencies of COD and UV_{254} absorbance were systematically investigated, and the effects of key operational parameters (pH, reaction time, current density, and temperature) were optimized using RSM. Additionally, toxicity analyses were conducted under optimized conditions, providing a comprehensive assessment of both environmental and removal efficiencies. The findings indicate that studies conducted on real pharmaceutical wastewater provide more holistic and practical results compared to analyses based on specific contaminants only, thus strengthening the potential of AOPs in industrial-scale wastewater treatment.

2. Materials and methods

2.1. The characterization of real pharmaceutical industry wastewater

Pharmaceutical wastewater was sourced from a manufacturing facility located in Tekirdağ, Türkiye. To prevent biological degradation, the samples were immediately stored at 4 °C until further analysis. The chemical oxygen demand (COD) (SM5220), UV_{254} (5910B), biochemical oxygen demand (BOD_5) (SM5210B) and pH (SM4500) of the wastewater were analyzed according to Standard Methods [28]. The real wastewater sample was characterized prior to treatment. The pH was measured as 6.73, indicating a slightly acidic medium. Electrical conductivity was found to be 73.90 mS/cm, reflecting a high ionic content. The UV_{254} absorbance was 1.68 cm^{-1}, suggesting the presence of significant amounts of aromatic organic compounds. Moreover, the COD and BOD_5 were determined to be 10,396 mg/L and 520 mg/L, indicating a substantial organic load in the wastewater. For pH adjustments during experiments, sodium hydroxide (NaOH, CAS 1310-73-2) and sulfuric acid (H_2SO_4, 95–97 %, CAS 7664-93-9) were used, both supplied by Merck.

2.2. Preparation of Ag/TiO_2 electrodes

The sol-gel method was used for the synthesis of Ag-doped TiO_2 (Ag/TiO_2) using titanium (IV) isopropoxide (TTIP) as a titanium precursor [29]. Initially, 25 mL of TTIP and 0.5 g of silver nitrate ($AgNO_3$, CAS 7761-88-8) were added dropwise to 500 mL of deionized water under continuous stirring to ensure controlled hydrolysis and homogeneous distribution of Ag ions. 5 mL of acetic acid (CH_3COOH) and 3.5 mL of nitric acid (HNO_3) were added to promote gel formation and stabilize the sol. The solution was then heated to 80 °C and stirred for 30 min to promote hydrolysis and condensation. After stopping the heating, the solution was stirred for another 2 h to ensure homogeneous sol stabilization. 316 stainless steel (2 × 6 cm in size and 0.1 mm thickness) material was used as an electrode. Before coating, the electrodes were sanded with paper sandpaper and cleaned using 0.1 M H_2SO_4. The cleaned electrodes were placed in the prepared sol gel and the entire surface was covered.

The deep coating method was used to deposit Ag/TiO_2 nanoparticle layers onto the electrode surfaces. The electrodes were completely immersed in the sol and withdrawn at a controlled rate to ensure uniform film deposition. To obtain a well-adhered and uniform coating, the deep coating process was repeated 10–15 times, resulting in a gradual increase in film thickness and improved surface coverage. After the final coating cycle, the electrodes were dried under a fume cupboard at room temperature and then calcined at 400 °C for 6 h, resulting in the formation of a photoactive nanostructured film with improved optical and charge-carrying properties. A schematic representation of the synthesis and coating process is given in Fig. 1.

In the present study, commercial 316 stainless steel electrodes were coated with Ag doped TiO_2 using the sol gel dip coating method, which is widely applied in photocatalytic material synthesis. Although SEM, XRD, and EDX analyses are commonly used to confirm surface morphology, crystal structure, and elemental composition, these characterizations were not performed in this study. The focus of the research is not the development of new materials, but the evaluation of the environmental performance of the coated electrodes in terms of COD and UV_{254} removal and toxicity reduction during advanced oxidation processes. The materials and synthesis procedure strictly followed established protocols reported in previous studies, where Ag doped TiO_2 coatings have been thoroughly characterized. These studies consistently report dominant anatase phase, uniform surface distribution, and stable silver incorporation, which are essential for photocatalytic performance [30–38].

To ensure the structural stability of the Ag-based electrode coatings and to exclude the possibility of silver leaching under intensified electrochemical conditions, a control analysis was performed. Aqueous samples collected after treatment at the highest applied current densities were analyzed for silver content using Inductively Coupled Plasma Atomic Emission Spectrometry (ICP-AES), following Standard Methods 3120 B. The results revealed no detectable silver in the treated effluent, indicating that the Ag layer remained chemically and mechanically stable throughout the process. This confirms that the system does not pose a secondary contamination risk due to electrode degradation, even under aggressive operational parameters.

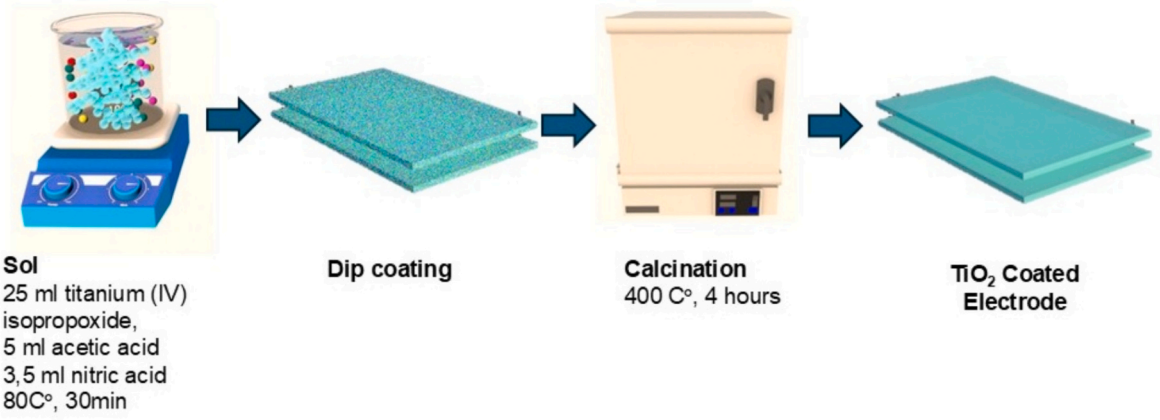


Fig. 1. Sol gel preparation and electrode coating process.

2.3. Experimental setup

Photoelectrochemical experiments were carried out in a custom-designed batch reactor made of quartz glass with inner dimensions of 10 cm × 10 cm × 5 cm. The reactor housed vertically aligned parallel plate electrodes with an inter-electrode gap of 0.5 cm. Inert spacers were placed between the electrodes to maintain fixed separation and prevent short-circuiting during electrolysis. The anode was fabricated from Ag-doped TiO_2-coated stainless steel, while the cathode consisted of TiO_2-coated stainless steel to ensure electrochemical stability and to prevent metal leaching observed in preliminary trials with uncoated stainless-steel electrodes.

In preliminary ECO and PECO trials, stainless steel electrodes were initially employed as cathodes due to their widespread use and availability. However, during extended operation under applied current, noticeable iron leaching from the cathode into the treated water was observed. This phenomenon was evidenced both visually, through a distinct yellowish discoloration of the solution, and analytically, indicating the release of Fe species likely resulting from cathodic corrosion processes. To overcome this issue and maintain system integrity, stainless steel electrodes coated with a thin layer of TiO_2 were subsequently used as cathodes. The application of this coating effectively prevented iron dissolution, as confirmed by the absence of color change and the lack of detectable iron in solution throughout the treatment process. Therefore, the use of TiO_2-coated stainless steel as the cathode was selected to ensure chemical stability and to avoid secondary contamination that could interfere with process performance and analytical evaluations.

The electrical current was supplied using a DC power source (Manson, 1–36 VDC, 10 A), which allowed precise control over the applied voltage and current throughout the treatment process. Illumination was provided by a single 40 W UV lamp positioned 2 cm directly above the reactor. Although only one light source was used, the interior walls of the light-proof enclosure housing the reactor were lined with aluminum foil to enhance light distribution through reflective scattering. The dimensions of the enclosed chamber were 40 cm × 50 cm × 60 cm, ensuring effective isolation from ambient light and facilitating uniform irradiation of the reactor.

Temperature control was achieved with a magnetic stirrer-hotplate system equipped with a feedback-controlled temperature probe immersed directly in the reaction solution. This allowed for real-time temperature monitoring and ensured thermal consistency across all experimental runs. Continuous stirring was employed to maintain homogeneity of the solution and uniform exposure of contaminants to the reactive surfaces.

This setup was specifically designed to optimize electrochemical and photo-driven reactions while addressing potential sources of variability such as electrode degradation, uneven light distribution, and thermal fluctuations. The schematic representation of the system designed in this study is presented in Fig. 2.

2.4. Toxicity analysis

Acute toxicity tests were conducted using *Daphnia magna*, following the OECD 202 guideline [39] to evaluate the toxicity of both raw and treated pharmaceutical wastewater. A series of wastewater dilutions were prepared at 100 % (raw wastewater), 90 %, 80 %, 50 %, 10 %, 5 %, and 1 % to assess toxicity variations at different concentrations. The pH of each sample was adjusted to above 8.0 using 1 M NaOH to ensure consistency across test conditions.

For each dilution ratio, 500 mL test solutions were prepared and transferred into glass beakers, each containing 20 *Daphnia magna* individuals. To maintain optimal test conditions, an air pump was utilized to sustain a dissolved oxygen level of 6 mg/L, while the temperature was controlled at 23 °C. The exposure conditions were standardized under an 18:6 h light-dark cycle with an illumination intensity of 3000 lx. Throughout the 24-h experimental period, no food was provided for the test organisms, as per standard acute toxicity test protocols. At the end of the 24-h exposure period, the number of immobilized *Daphnia magna* individuals was recorded to determine the toxicity levels of each wastewater dilution.

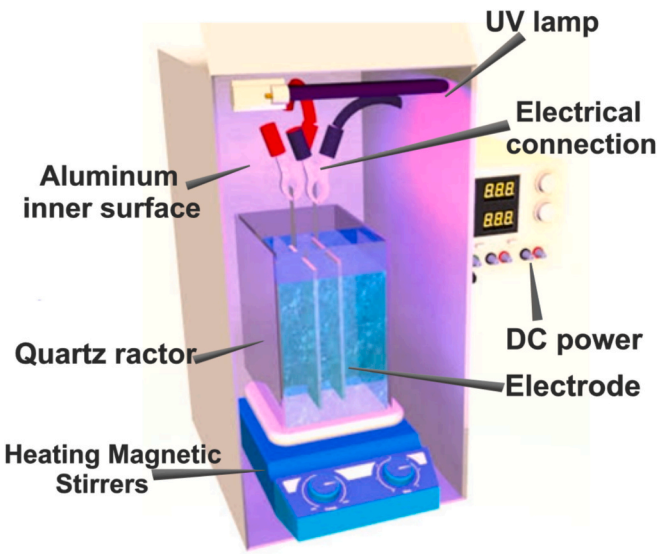


Fig. 2. Schematic representation of the PECO and ECO system.

2.5. Analytical methods

UV_{254} measurement is a crucial parameter for assessing the concentration of natural organic matter and aromatic compounds in water. This measurement is particularly used in water treatment processes to estimate the potential formation of disinfection by-products and to monitor the level of organic pollution in water [40,41]. UV_{254} results were spectrophotometrically measured by collecting samples before and after the treatment process. Removal efficiencies were calculated based on Eq. (1).

$$\eta_{removal} = \left(\frac{A_0 - A_t}{A_0}\right) * 100 \quad (1)$$

where, $\eta_{removal}$ is treatment efficiency rate (%), A_0: the initial absorbance value, A_t: initial absorbance value at time t.

Chemical Oxygen Demand (COD) is a key analytical parameter used in the assessment of water quality, as it indicates the extent of organic pollution present in aquatic environments [42,43]. The COD of samples collected before and after the treatment process was determined according to the standard method (SM5220). COD removal efficiency was calculated based on Eq. (2).

$$\eta_{removal} = \left(\frac{C_0 - C_t}{C_0}\right) * 100 \quad (2)$$

where, $\eta_{removal}$ is treatment efficiency rate (%), C_0: the initial pollutant concentration, C_t: pollutant concentration at time t.

2.6. Response surface methodology (RSM)

In experimental studies, traditional multi-factor optimization is typically conducted by keeping other factors constant while evaluating the effect of a single variable. However, this approach fails to fully capture the interactions between factors and often leads to unnecessary time and chemical consumption. To overcome these limitations and enable a more systematic analysis, this study employs Response Surface Methodology. RSM facilitates process optimization by mathematically modeling the interactions between independent variables and the response variable. Additionally, classical optimization methods have been evaluated alongside model-based optimization results to enhance the accuracy of the optimization process through comparative analyses. Among the widely used experimental design approaches for determining optimal operating conditions are CCD, BBD, and two-level full factorial design methods.

CCD is widely used optimization methods in RSM. This method offers an efficient approach to experimental design by requiring a minimal number of tests, incorporating a standard 2^n factorial design at the center point, 2^n axially fixed points at an alpha distance, and replicating tests at the center [44]. Response surface methodology employs a mathematical function to fully model the relationship between dependent and independent variables, this function is usually expressed as in Eq. (3)

$$Y = f(x_1, x_2, \ldots x_n) + \mathcal{E} \quad (3)$$

In this equation, Y represents the response variable, X denotes the independent variables, n is the number of factors, Ɛ accounts for the model error, and f represents the unknown response surface function. This systematic approach provides a powerful tool for determining optimal operating conditions and accurately analyzing the effects of process parameters on the response variable.

RSM operates using the coded values of the process variables defined within the study. The relationship between the actual values of these variables and their corresponding coded values is represented by Eq. (4) [45].

$$Coded\ value = X_i = \frac{X_i - X_{av.}}{\Delta X} \quad (4)$$

Here, X_i; represents the actual value of factor, X_{av} is the average of the lowest and highest values of factor, and ΔX is change between two values. To accurately model the relationship between the independent variables and the response, a second-order polynomial equation is employed. This approach allows for the identification and interpretation of linear, quadratic, and interaction effects of the variables on the response. Such equations, commonly referred to as RSM, are typically first- or second-degree polynomial functions [46–51] (Eqs. (5), (6)).

First-Degree Model

$$Y = \beta_0 + \sum_{i=1}^{n} \beta_i X_i + \varepsilon \quad (5)$$

Second-Degree Model

$$Y = \beta_0 + \sum_{n=1}^{k} \beta_n . x_n + \sum_{n=1}^{k} \beta_{nn} . x_n^2 + \sum_{n \le m}^{k} \sum_{m}^{k} \beta_{nm} . x_n x_m + \ldots . e \quad (6)$$

The regression coefficients βi, βii, βij, i, j, n are indices, are used to express the relationship between the factors and the response.

The first-degree model represents a linear surface, whereas the second-degree model also known as the quadratic model describes a curved surface that incorporates linear, quadratic, and interaction terms. This quadratic model offers a comprehensive and reliable framework for predicting responses within the scope of RSM. In this study, experimental design, data analysis, and optimization of the independent process variables are conducted using CCD in conjunction with RSM.

The experimental design was based on a four-factor, five-level central composite design (CCD), in which pH (A), reaction time (B), applied current (C), and temperature (D) were selected as the independent variables. Each variable was coded at five levels (−2, −1, 0, +1, +2), corresponding to the actual values used during the experiments. The pH levels ranged from 3 to 11, reaction time varied between 15 and 75 min, current was applied in the range of 0.2 to 1.0 A, and the temperature was adjusted from 20 to 60 °C. Detailed coded and actual levels of each factor are provided in Table S1.

3. Result and discussion

3.1. Regression models and statistical analysis

The accuracy of model prediction is commonly assessed using the coefficient of determination (R^2). A model with strong predictive capability typically exhibits an R^2 value close to 1. However, as the number of terms included in the model increases, the R^2 value may also increase regardless of whether those additional terms are statistically significant. Therefore, relying solely on the R^2 value can be misleading. To more accurately evaluate the model's predictive performance, it is essential to consider the adjusted R^2 value, which accounts for the number of predictors in the model and provides a more reliable measure of goodness-of-fit. [52].

In the statistical analysis of the PECO process (Ag/TiO_2-TiO_2), the R^2 for COD and UV_{254} removal efficiencies were found to be 98.87 % and 99.34 %, respectively, while the adjusted R^2 values were 97.81 % and 98.73 %. A large discrepancy between the R^2 and adjusted R^2 values is not desired for model adequacy [53]. These coefficients are a measure of how well statistical models predict the output [54]. The results are consistent with the R^2 values reported in similar studies in the literature, supporting that the method can generate predictive models with high reliability [55]. As shown in Tables S4, S7, S10, and S13 the difference between the R^2 and adjusted R^2 values for all responses is minimal.

The coefficient of variation (CV) is used to express the repeatability characteristic of a model, and a CV value below 10 % indicates that the

model is repeatable [53]. The CV values obtained for COD and UV_{254} removal efficiencies in the model are 3.95 % and 3.24 %, respectively, both of which are below 10 %. The adequate precision (AP) should exceed a value of 4 for model adequacy [56]. High AP values demonstrate the accuracy of the developed models. The AP values for COD and UV_{254} removal efficiencies, which are >4, are shown in Tables S4, S7, S10, and S13.

The model F-values obtained for COD and UV_{254} removal in the PECO process were 93.51 and 161.92, respectively. These values indicate that the developed models are statistically significant and demonstrate an ideal correlation between the independent variables and the responses [57]. Another indication of the models' significance is that the *p*-values obtained for all models are below 0.05. The corresponding p-values for the F-values ($p < 0.0001$) validate the developed mathematical models. Additionally, the Sum of Squares values for all models were found to be high. Another parameter used to test model adequacy is the model inconsistency value based on repeated measurements. The model inconsistency *p*-values for all four models were found to be >0.05, indicating that the model inconsistency is not statistically significant [58]. According to the ANOVA results, the significance of each linear, quadratic, and interactive parameter is evaluated. For COD and UV_{254} removal, all linear parameters are found to be significant. The factors are compared based on their F and *p*-values at a 95 % confidence level. A higher F value and a lower p-value indicate that the corresponding coefficient is more significant [59]. Based on the F and p-values, the most significant linear parameter for COD and UV_{254} removal is found to be the current (Tables S2, S5, S8, S11).

The data obtained from the experimental sets shown in Table S1 were used for model optimization. The results obtained under the conditions applied to the coded factors were used to run and generate correlation equations, which are presented in Tables S14, S15, S16, and S17.

Normal probability plots and predicted versus actual plots were employed to evaluate the correlation between experimental and model-predicted values (Fig. S1). The scatter of the predicted and actual data around the 45-degree line demonstrates that the error between the actual and predicted values is very low. These graphs indicate that the proposed models exhibit a high correlation and that the models have strong predictive capabilities for COD and UV_{254} removal in the ECO and PECO processes. Based on the obtained results, it can be concluded that the developed models are applicable for determining the optimal process conditions that would result in the highest COD and UV_{254} removal efficiencies.

3.2. *Effect of process variables (temperature, time, current, pH)*

Four Pareto charts comparatively show the effect of process variables on COD and UV_{254} removal efficiencies for both PECO and ECO systems (Fig. S2). In all cases, variables C and D consistently exhibit the highest frequency, indicating their dominant roles in the performance of both processes. For COD removal, the PECO process shows a higher contribution from interaction terms (27 %) compared to ECO (20 %), indicating a more complex system behavior affected by the synergistic effects between variables. Similarly, for UV_{254} removal, interaction effects account for 33 % in PECO, while this value drops to 27 % in ECO, with a higher dominance of first-order terms (46 %).

From a statistical point of view, the dominance of linear effects indicates that most of the variability of the system can be explained without the need for complex nonlinear or interaction models [60]. This not only facilitates interpretation but also increases the robustness and practical applicability of the developed model. The relatively small contributions of quadratic and interaction terms indicate that the curvature of the response surface and the synergistic effects between variables are negligible or of secondary importance. Therefore, focusing on the optimization of linear parameters can lead to significant improvements in process efficiency while maintaining model simplicity and reducing computational complexity.

These findings indicate that PECO is governed by more complex relationships between parameters, while ECO follows a more linear and individually driven pattern. Compared to PECO, the ECO process shows a simpler structure, where individual operating parameters mainly determine the removal performance. In all four cases, >80 % of the total effect is explained by the first six to seven terms, confirming the power and reliability of the models. In general, PECO requires a more comprehensive optimization strategy considering multi-factor interactions, while ECO offers a simpler and more predictable path for process control and operational efficiency.

The effects of initial pH, reaction time, current density, and temperature on COD and UV_{254} removal in the PECO process were determined using the Central Composite Design (CCD) method. The results obtained provide important data for process optimization by graphically illustrating the interactions of the variables (Fig. 3).

The findings show that pH is a decisive factor for COD removal. Specifically, COD removal is more efficient in a neutral environment (pH 6–7), while the removal efficiency significantly decreases under alkaline and acidic pH conditions (Fig. 3). On the Ag/ TiO_2 surface, both the photocatalyst and organic molecules become positively charged, which increases electrostatic repulsive forces, thereby reducing adsorption and, consequently, degradation efficiency [61,62]. This phenomenon explains the decrease in removal efficiency to 20–40 % in the pH range of 9–11.

A significant decrease in removal efficiency was observed with the increase in temperature. At pH 7, increasing the temperature from 20 °C to 60 °C led to a reduction in COD removal from 85 % to 62 %. This can be explained by the fact that at high temperatures, the catalyst's adsorption capacity increases, reducing the photocatalytic surface area and consequently limiting the formation of ROS [63]. The results indicate that optimal treatment conditions are achieved at lower temperatures, and that an increase in temperature may have a negative impact on photocatalytic processes.

When the interaction between processing time and current density was examined, it was found that an increase in both the processing time and current density significantly improved COD removal. High current densities have a stronger effect on UV_{254} removal compared to COD removal by increasing the production of hydroxyl radicals [64]. Furthermore, the combination of photochemical reactions with electrochemical oxidation creates synergistic effects that accelerate the degradation of resistant compounds [65]. However, excessively high current densities can lead to degradation of the catalyst surface, mass transfer limitations, and reduced electrode stability [66]. Therefore, both efficiency and long-term operating stability should be considered when determining the optimum current density.

Similarly, as the processing time increased, improvements in COD and UV_{254} removal efficiency were observed. Specifically, at 60 °C, increasing the processing time from 15 min to 75 min raised the removal efficiency from 40 % to 80 %. Longer irradiation times generally lead to higher pollutant removal rates [67]. However, the optimal processing time in these processes depends on factors such as the initial pollutant concentration, photocatalyst dosage, and reactor conditions. To evaluate the applicability of the process at an industrial scale, the design of photocatalytic reactors must be carefully optimized with respect to processing time, light source, and treatment capacity [68].

This study comprehensively investigates the optimization of PECO process, focusing on the effects of four key variables pH, reaction time, current density, and temperature on COD and UV_{254} removal efficiencies. The results reveal that higher removal efficiencies are achieved under neutral pH and 20 °C temperature conditions. Additionally, increased current densities enhance removal efficiency by boosting the production of ROS; however, excessively high current densities may negatively impact electrochemical stability, leading to catalyst surface deterioration. These findings underscore the effectiveness of combining photo-chemical and electrochemical processes in tackling resistant

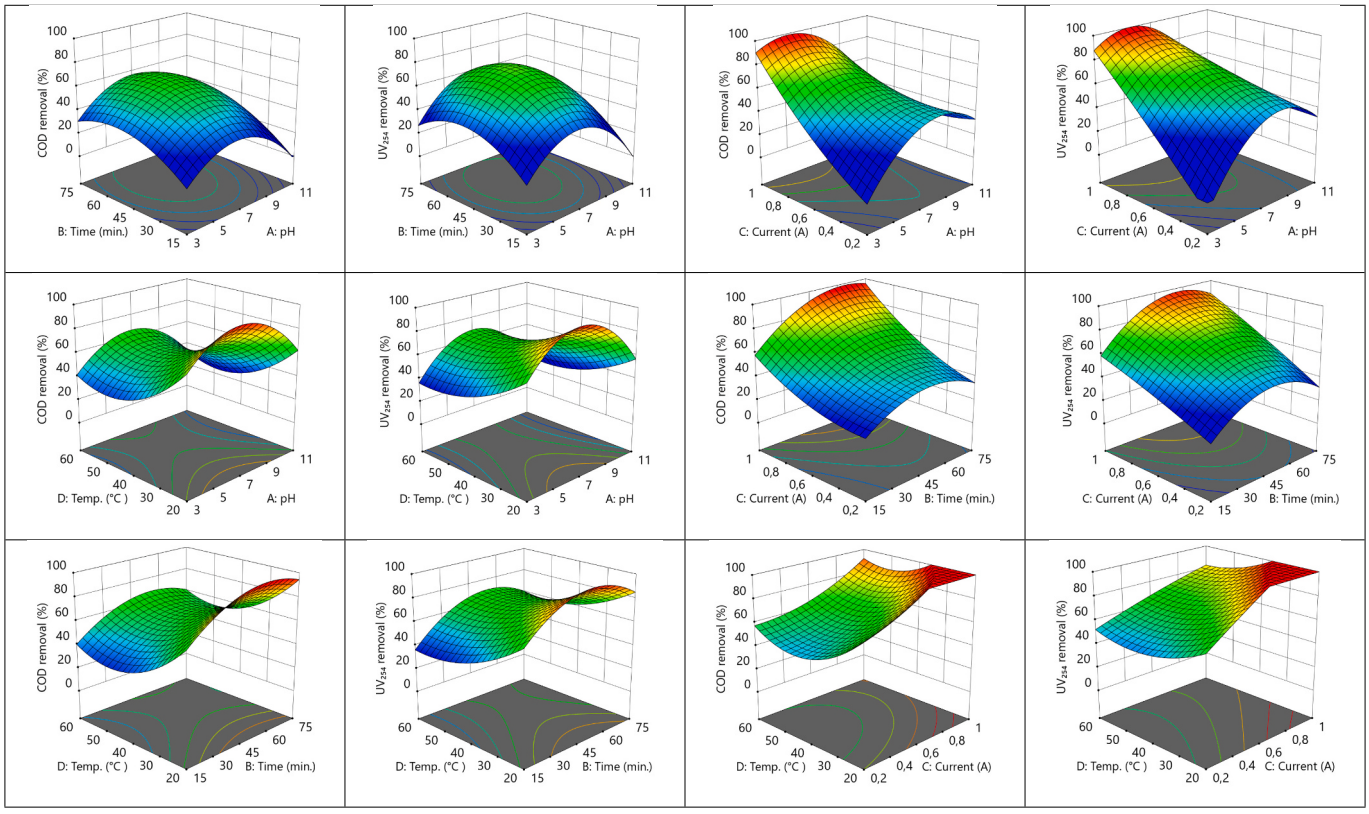


Fig. 3. 3D graphs of COD and UV_{254} removal by PECO process.

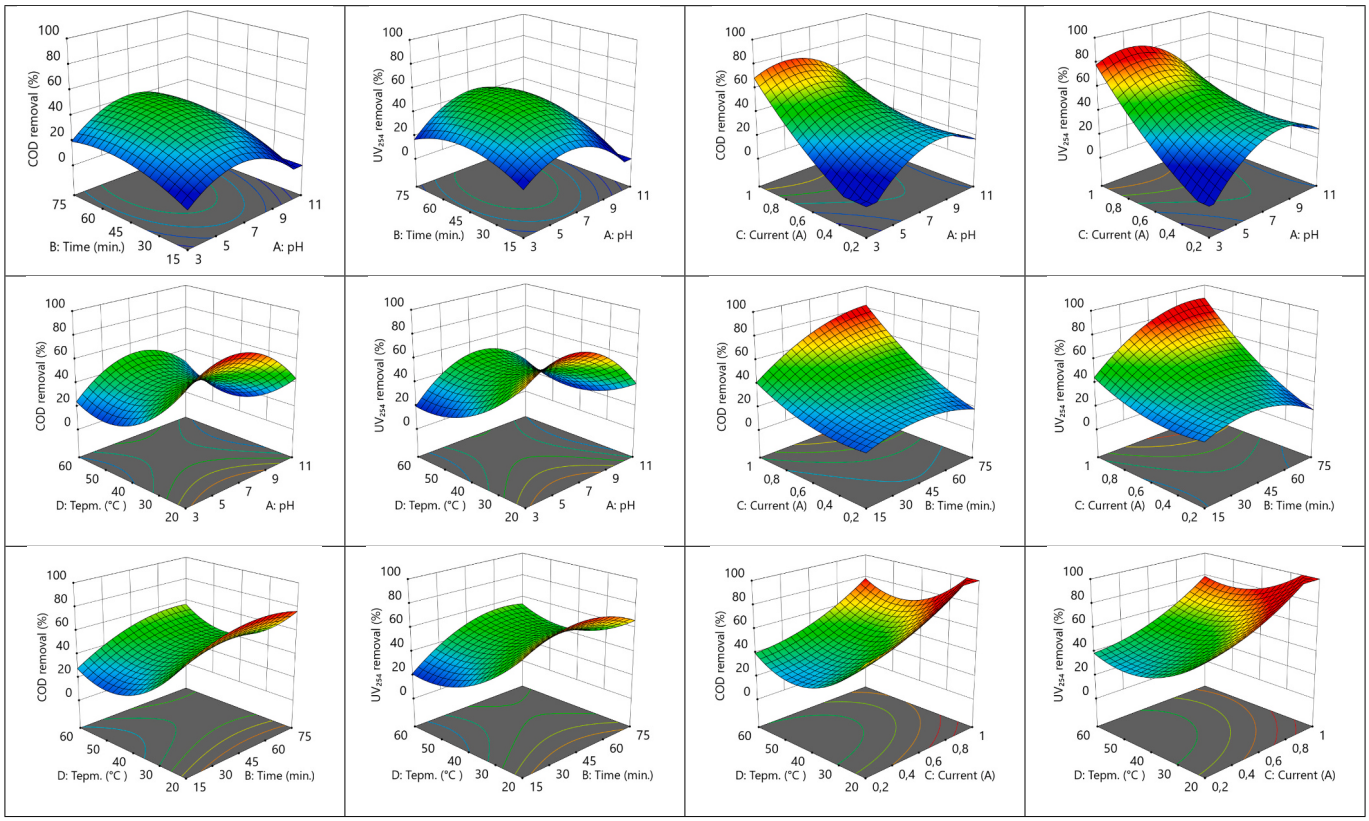


Fig. 4. 3D graphs of COD and UV_{254} removal by ECO process.

organic pollutants. Furthermore, this study emphasizes the critical need for carefully optimizing process parameters to ensure long-term operational stability and high efficiency, especially when considering the potential for industrial-scale applications.

The performance of an Ag-doped TiO_2 anode coupled with a TiO_2 cathode was systematically evaluated in an ECO system for the removal of COD and UV_{254} absorbing compounds. The effects of four key parameters pH, temperature, current intensity, and reaction time on COD and UV_{254} were investigated. As illustrated in Fig. 4, 3D surface plots were employed to visualize the impact of each parameter, highlighting the strong correlation between COD and UV_{254} removal.

Among the parameters studied, reaction time was found to have a significant influence on removal efficiencies. As the duration increased, both COD and UV_{254} removals improved notably. Under high current conditions, 75 min of operation resulted in COD removal of up to 85 % and UV_{254} removal nearing 95 %. This improvement can be attributed to the extended interaction time between reactive species and organic pollutants, which enhances the oxidation process. However, under low current conditions (below 1.0 A), treatment had an adverse effect on UV_{254} removal. This decline may be linked to the accumulation of intermediate by-products on the electrode surface, which can inhibit further oxidation [69].

These findings underscore the important role of current intensity in the system's overall performance. At the current level of 1.0 A, maximum removal efficiencies were achieved 90 % for COD and 95 % for UV_{254}. Particularly for UV_{254}, which reflects the presence of aromatic structures, the degradation was more efficient under elevated current. This enhanced removal is attributed to the increased generation of OH•, which plays a central role in breaking down recalcitrant aromatic compounds [70].

In addition to current and time, the pH of the reaction medium also played a critical role in system efficiency. Optimal removal rates for both COD and UV_{254} were observed in the near-neutral range (pH 4–7), while performance declined under strongly acidic or basic conditions. Interestingly, at pH 9, a slight increase in UV_{254} removal was recorded, which may be associated with the elevated concentration of OH^- ions. These ions can promote redox reactions and enhance radical generation, partially compensating for the overall decline in system efficiency at high pH [71].

The influence of temperature, on the other hand, presented a different trend. High removal efficiency was observed for both parameters at lower temperatures (20–25 °C). However, as the temperature increased, COD removal efficiency declined significantly, whereas UV_{254} removal remained relatively stable. This divergence suggests that while COD removal is sensitive to temperature, the degradation of UV_{254} active compounds is more strongly governed by radical availability and current density than by thermal activation [70,72].

The maximum COD removal efficiency obtained under the standard experimental conditions was 76 %, corresponding to a final COD concentration of 2495 mg/L, which remains above the permissible discharge limits for pharmaceutical wastewater. While this value was recorded after 30 min of treatment, extended operation under the same conditions led to significantly higher removal rates. As presented in Table S9, the PECO process achieved over 98 % COD removal at 60 min, indicating that the discharge standards can be met when sufficient treatment time is provided. However, increasing the reaction duration also raises energy consumption, which may challenge the cost-effectiveness and scalability of the process in industrial applications.

Considering these trade-offs, the system is better suited for use as a pretreatment stage. Both ECO and PECO significantly reduced effluent toxicity and increased the COD to BOD_5 ratio, suggesting that persistent and toxic compounds were partially converted into biodegradable forms. These enhancements in effluent quality can facilitate more efficient downstream biological treatment. Therefore, integrating the proposed process prior to biological systems presents a more feasible and sustainable solution for pharmaceutical wastewater management, particularly under real-world operational constraints.

Taken together, these results confirm that the Ag-doped TiO_2 assisted ECO system is highly effective in removing both total organic matter and UV_{254} active pollutants, with both indicators generally following similar trends.

3.3. Degradation and mineralization performance of ECO and PECO systems

The comparative evaluation of the ECO and PECO systems, as illustrated in Fig. 5, reveals critical insights into their pollutant degradation behavior and mineralization capacity. Both systems demonstrated a rapid decline in TOC, UV_{254}, and color during the initial 15 min of treatment, followed by a slower and more gradual trend towards equilibrium. This pattern indicates that initial removal is governed by surface oxidation and bulk-phase diffusion, while later stages are controlled by slower electron transfer and degradation of intermediate compounds.

In the ECO system, TOC removal efficiencies stabilized around 75 to 78 % for both Ag/TiO_2-TiO_2 and TiO_2-Ag/TiO_2 configurations. Although UV_{254} and color removal were also satisfactory, final values remained below 80 %, with color removal in particular remaining under 68 % for the TiO_2-Ag/TiO_2 configuration. This suggests that while partial oxidation occurs, complete mineralization and disruption of chromophoric structures are limited without the assistance of photogenerated oxidants. These results underline the challenges associated with degrading high molecular weight organic compounds through electrochemical processes alone.

In contrast, the PECO system achieved significantly higher removal efficiencies across all measured parameters. TOC removal exceeded 85 % in the Ag/TiO_2-TiO_2 configuration, with similar performance observed for TiO_2-Ag/TiO_2. Notably, substantial reductions in UV_{254} and color were observed, indicating efficient cleavage of aromatic and chromophoric structures. The continued improvement beyond 60 min particularly in TOC and color suggests ongoing generation of reactive oxygen species and deeper oxidation pathways becoming active during the process.

To complement efficiency data, normalized concentration values (C/C_0) were evaluated. The PECO system reduced C/C_0 values for TOC and UV_{254} to below 0.2 within 120 min, corresponding to over 95 % removal of organic content. These results reflect not only structural transformation but also strong mineralization, with organic matter being fully converted into inorganic end products. The steady decline in UV_{254} absorbance reflects breakdown of aromatic structures, while complete color removal confirms degradation of complex dye molecules into non-chromophoric or fully oxidized species.

The ECO system also exhibited gradual pollutant degradation, though with relatively slower kinetics and higher final concentrations. This can be attributed to the absence of UV-induced charge carrier excitation, which limits the formation of highly reactive species such as hydroxyl radicals. Despite this limitation, ECO remains a viable option for partial oxidation, especially in applications where energy input is constrained.

Taken together, the combined analysis of removal efficiencies and normalized concentrations confirms that the PECO configuration achieves deeper and more effective mineralization compared to ECO. The synergy between photochemical and electrochemical processes promotes not only rapid degradation but also complete mineralization of recalcitrant pollutants. This demonstrates the potential of PECO as a promising and robust treatment strategy for complex and toxic wastewater streams requiring advanced oxidation.

3.4. Validation analysis

The contour plots based on the desirability function are uniquely generated for each study, as they are directly derived from the experimental model and response behavior specific to the investigated system.

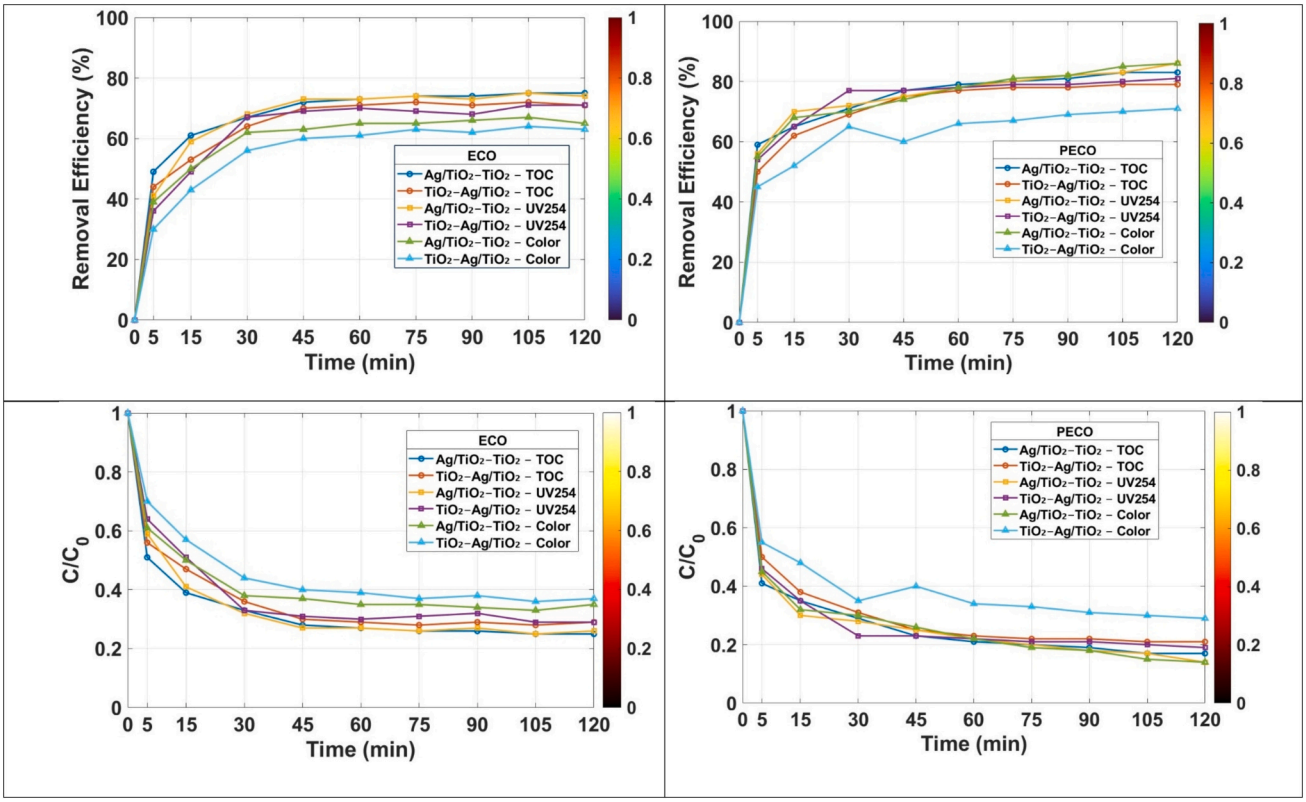


Fig. 5. Comparison of removal efficiencies ande C/C_0 for TOC, UV_{254}, and color parameters under ECO and PECO conditions using Ag/TiO_2-TiO_2 and TiO_2-Ag/TiO_2 electrode configurations (All experiments were conducted at pH 5, 0.8 A current, and 30 °C).

In this work, the desirability plots corresponding to the present process are shown in Fig. 6. These graphical tools enabled the identification of optimal operating conditions by revealing the interactions between key variables pH, current, reaction time, and temperature.

Through the interpretation of these desirability plots, the combination of input variables that maximize the overall process performance was successfully determined. Notably, the visual representation of desirability across variable ranges provided valuable insight into the nonlinear and interdependent effects of the operating parameters. This comprehensive analysis allowed for the exclusion of conditions that might appear suitable in single-factor evaluations but result in reduced process efficiency when interactions are considered [54].

Following the optimization step, validation experiments conducted under the predicted optimum conditions to verify the accuracy and robustness of the model. Table 1 presents the impact of process optimization and various electrode pairings on COD and UV_{254} removal under optimal conditions. The strong correlation between predicted and experimental values in both methods indicates a high level of model reliability and predictive performance [73]. The ECO method achieved effective oxidation with a performance of 70 % COD removal and 68 % UV_{254} removal. However, the PECO method, particularly with the Ag/TiO_2-TiO_2 electrode pair and the contribution of UV light, demonstrated higher performance, achieving COD and UV_{254} removal efficiencies of 76.80 % and 86.03 %, respectively. It was observed that using the Ag/TiO_2 electrode as the anode was more suitable than using it as the cathode. The results indicate that PECO, due to its photocatalytic activity, is more efficient than ECO.

The relative errors between the predicted and actual values ranged from 0.14 % to 3.22 %, indicating a high level of agreement (Table 1). These low error margins demonstrate the robustness and predictive reliability of the model across both COD and UV_{254} removal efficiencies under identical operational conditions. Notably, the relative errors below 1 % further confirm the model's ability to closely replicate experimental outcomes. Such accuracy is particularly valuable for process optimization and real-time control in advanced oxidation systems, suggesting that the developed model can serve as a practical and efficient tool for performance forecasting in electrochemical and photoelectrochemical treatment applications.

Table 1 presents a comparative analysis of ECO and PECO systems using two different electrode configurations: Ag/TiO_2-TiO_2 and TiO_2-Ag/TiO_2. The results indicate that, under identical experimental conditions (pH 5, 30 min, 0.8 A current, and 30 °C), there is no significant difference in the removal efficiencies between the two electrode arrangements in the ECO process. COD removal values for Ag/TiO_2 as anode and cathode were measured as 70.97 % and 69.87 %, respectively. Similarly, UV_{254} removal efficiencies were 68.71 % and 67.38 %. The relative errors remained low in both cases, suggesting a high degree of consistency in system performance.

This similarity may be attributed to the limited contribution of photonic activation in the ECO process since it is driven primarily by electrochemical oxidation rather than photocatalysis. Both configurations utilize TiO_2-coated surfaces that can facilitate oxidation reactions, and the absence of significant light influence in ECO minimizes the performance gap between the two orientations. Furthermore, under these conditions, the dominant mechanism is likely direct electron transfer and surface-mediated oxidation, where the relative position of the Ag-doped layer may not critically influence the reaction pathways.

In contrast, more pronounced differences are observed under PECO conditions, where UV irradiation plays a central role. These findings support the idea that electrode configuration becomes more critical in processes involving photoactivation, whereas in purely electrochemical systems, both orientations offer comparable oxidation efficiency.

A modest improvement in COD removal was observed when ECO was replaced by PECO using the Ag/TiO_2 anode, with a difference of approximately 7 % under the selected operational conditions. This value corresponds to the optimum conditions identified for short-duration

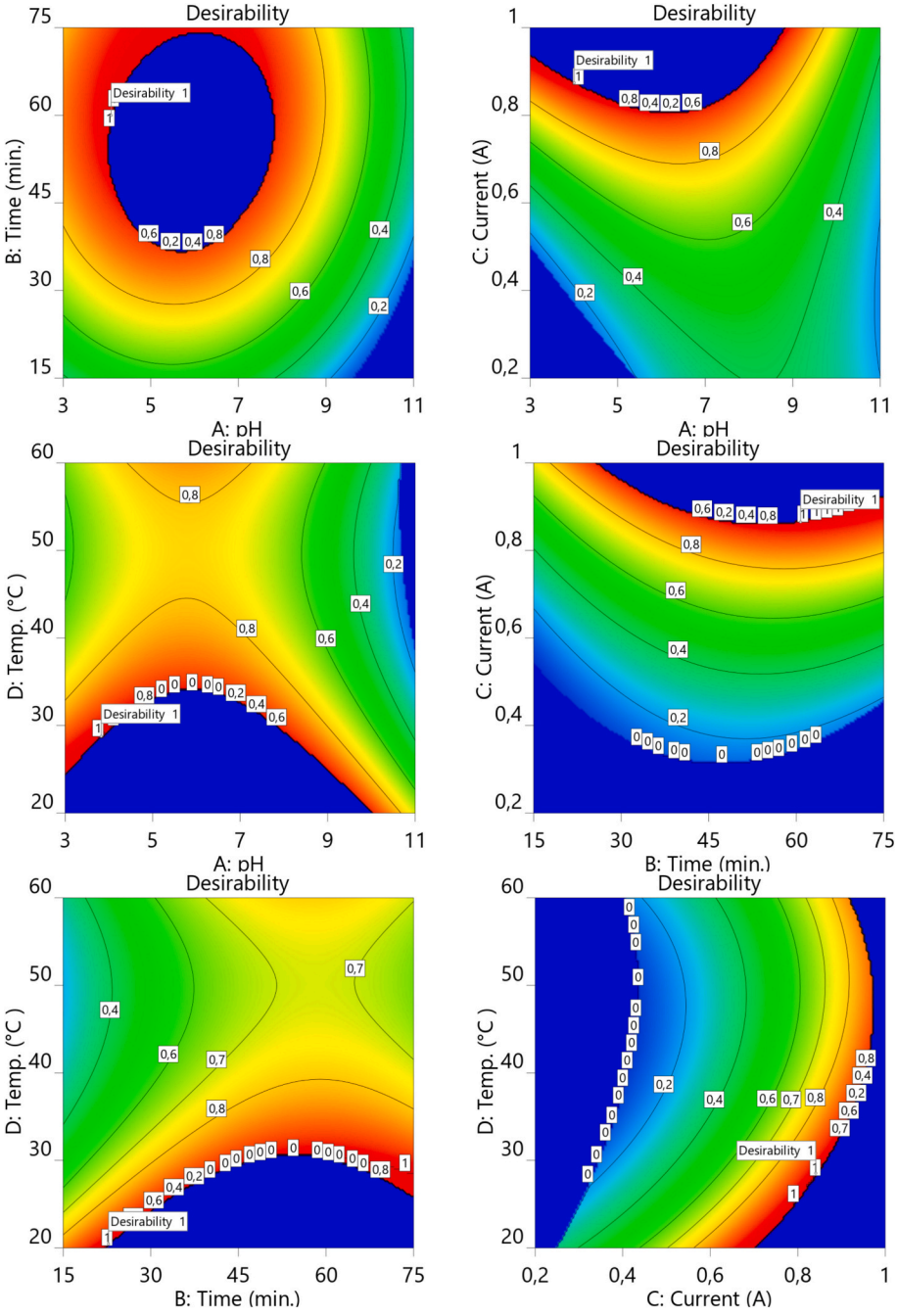


Fig. 6. Desirability surface plots showing optimal regions.

Table 1
Experimentally obtained, and model predicted results of PECO and ECO processes.

			Variables				Predicted Value	Actual Value	Relative error
			pH	Time	Current	Temp.	%	%	%
ECO	Ag/TiO_2-TiO_2	COD	5	30	0,8	30	71,52	70,97	0.77
		UV_{254}	5	30	0,8	30	69,12	68,71	0.60
	TiO_2-Ag/TiO_2	COD	5	30	0,8	30	71,54	69,87	2.39
		UV_{254}	5	30	0,8	30	69,12	67,38	2.58
PECO	Ag/TiO_2-TiO_2	COD	5	30	0,8	30	78,79	76,80	2.59
		UV_{254}	5	30	0,8	30	85,91	86,03	0.14
	TiO_2-Ag/TiO_2	COD	5	30	0,8	30	75,83	73,46	3.22
		UV_{254}	5	30	0,8	30	78,02	77,82	0.26

operation aimed at pretreatment applications, specifically a 30-min treatment period. Examination of broader experimental results presented in Tables S3, S6, S9, S12 reveals that the overall difference in COD removal efficiency between ECO and PECO systems can reach up to 20 %. This variation highlights the influence of process parameters such as pH, current density, temperature, and reaction time on system performance. Extended treatment durations enhance photocatalytic activation and increase the production of reactive oxygen species, which contributes to a more pronounced difference between the two systems.

The observed 7 % improvement under optimum pretreatment conditions reflects a deliberately selected balance between energy input and removal efficiency. In scenarios where higher removal rates are required to meet stringent discharge limits, longer treatment times and more intensive operating conditions would be necessary. Under such circumstances, the performance advantage of PECO over ECO becomes more evident, supporting its application in advanced oxidation processes that target deeper mineralization. These findings emphasize the importance of contextualizing performance metrics within the framework of treatment goals, operational constraints, and the intended role of the system within a larger treatment train.

3.5. *Photocatalyst recyclability and performance retention over multiple cycles*

A comparative evaluation of the C/C_0 profiles over six successive cycles demonstrated significant variations in degradation performance depending on the type of oxidation process (ECO vs. PECO) and electrode configuration (Fig. 7). It is important to note that all recyclability tests were performed under the optimized operational conditions (pH 5, 0.8 A current, 75 min reaction time, and 30 °C), which were identified through statistical optimization In the ECO system utilizing the Ag/TiO_2-TiO_2 electrode pair, substantial TOC removal was achieved during the first three cycles, with C/C_0 values decreasing below 0.25. However, from the fourth cycle onward, a gradual decline in removal efficiency was observed. This performance loss can be attributed to surface passivation and a reduction in the number of active sites, which are common limitations of electrochemical oxidation systems operating without photonic assistance [74].

The PECO system employing the same Ag/TiO_2-TiO_2 configuration exhibited superior and more consistent degradation efficiency across all six cycles. The improved performance is attributed to the synergistic effect between photogenerated electron-hole pairs and silver doping. The presence of Ag on the TiO_2 surface acts as an effective electron trap, enhancing charge separation and extending photocatalytic activity. UV irradiation accelerates the generation of reactive oxygen species while suppressing charge recombination, which is a critical factor in maintaining high oxidative potential during prolonged reuse.

In contrast, when the electrode configuration was reversed (TiO_2-Ag/TiO_2), a comparable degradation efficiency was observed in the first PECO cycle, but a more pronounced decrease occurred in subsequent cycles. This trend indicates that the position of Ag within the electrode architecture plays a pivotal role in ensuring optimal charge transfer dynamics and catalytic stability. The reduced exposure of the Ag-doped surface to UV light in the reversed setup may have limited the localized surface plasmon resonance (LSPR) effect, thereby diminishing the efficiency of photocatalytic reactions.

In the PECO system where the Ag/TiO_2-coated electrode functioned as the cathode, the overall degradation efficiency was lower than that of the other configurations. Nevertheless, the C/C_0 profiles across all six cycles remained closely aligned, indicating minimal variation in performance over time. This observation highlights the structural durability and reusability of the system. The silver doping not only enhanced the electronic conductivity and redox stability of the TiO_2 coating but also reinforced its mechanical and chemical integrity. These characteristics contributed to the preservation of the coating structure and maintained consistent system performance throughout repeated use.

However, based on observations from preliminary tests and consistent with previous studies, a decline in pollutant removal efficiency was

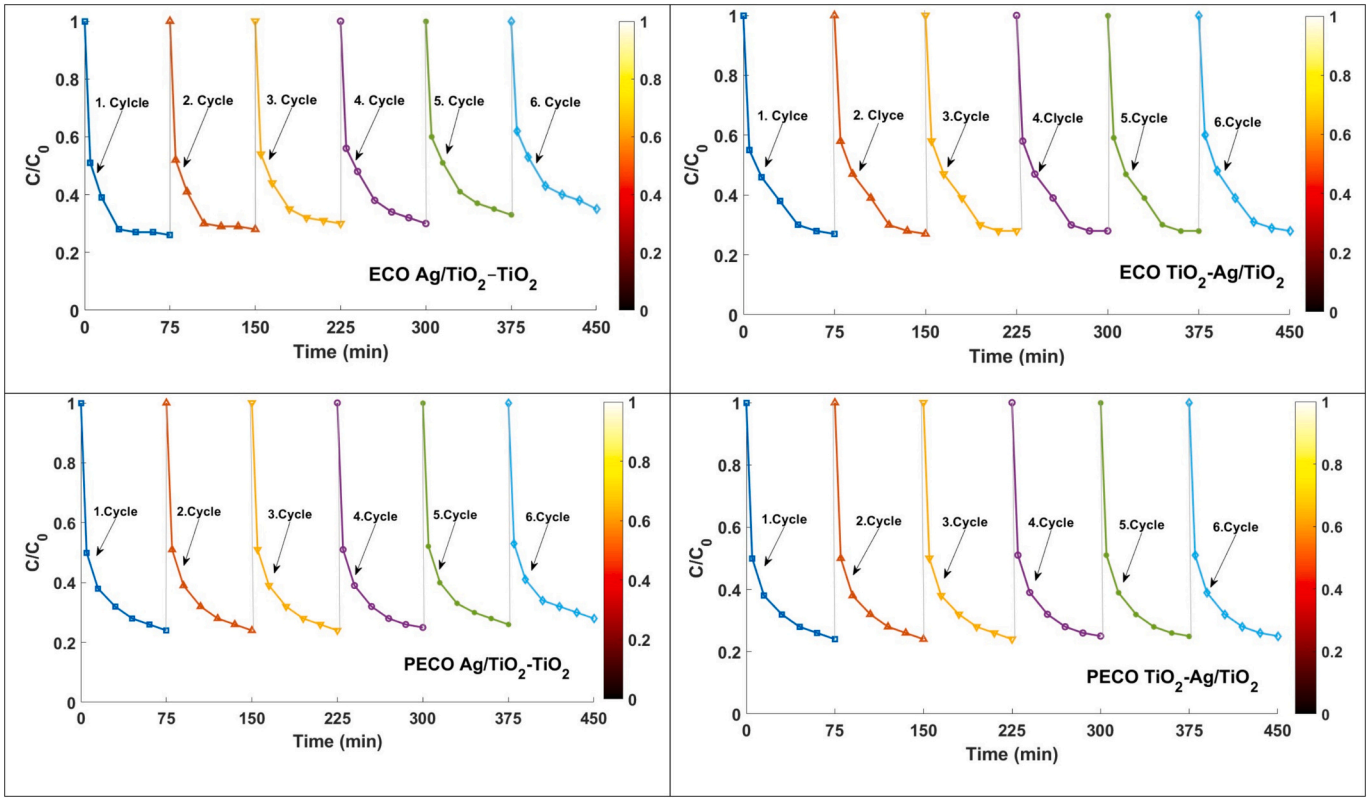


Fig. 7. Multi-cycle TOC Removal Efficiency of ECO and PECO Systems (pH = 5, Temperature = 30 °C, 0,5 A).

noted after approximately six reuse cycles. Therefore, to ensure reproducibility and sustained performance, the electrodes were recoated with fresh Ag/TiO_2 catalyst after every three experimental sets. This strategy minimized performance losses associated with catalyst detachment, surface fouling, or ROS activity degradation.

The results of this study provide important evidence regarding the reusability of Ag-doped TiO_2 electrodes in both electrochemical and photoelectrochemical systems, specifically for the treatment of real pharmaceutical wastewater. While numerous studies have reported the recyclability of Ag-TiO_2 photocatalysts, these have predominantly focused on synthetic dye solutions or textile effluents. For instance, Boxi et al. investigated the degradation of metronidazole using Ag-doped hollow TiO_2 and observed a 10.47 % decrease in photocatalytic performance after six reuse cycles [75–76]. The observed decline was attributed to the partial reduction of Ag^+ ions to metallic silver during photocatalysis, which suppressed the catalytic activity [77,78].

Similarly, high initial efficiencies have been reported in other dye-based systems, such as 90 % degradation of Methylene Blue, Methyl Red, or Crystal Violet within the first two cycles [77,78], 100 % removal of Methyl Orange after three cycles using 0.5 % Ag-TiO_2 [79], and 89 % efficiency after five cycles with 4.0 % Ag-TiO_2 in Methylene Blue degradation [80]. However, these systems typically operate under controlled conditions with synthetic matrices, and there is a lack of comprehensive reuse studies under real, pharmaceutically contaminated wastewater conditions.

In contrast, the current work demonstrates that Ag/TiO_2-TiO_2 electrodes can be reused for six consecutive cycles in the treatment of actual pharmaceutical effluent without requiring regeneration procedures between runs. Although some reduction in degradation efficiency was noted in specific configurations (e.g., when Ag/TiO_2 was used as the cathode), the differences in performance across cycles remained limited. This stable behavior is indicative of the strong interfacial interaction between Ag and the TiO_2 support, which likely enhances the mechanical and chemical durability of the coating. The minimal drop in efficiency over time suggests that silver doping not only improves the initial photocatalytic activity but also reinforces the adhesion and robustness of the TiO_2 layer. Importantly, the use of real wastewater rich in complex pharmaceutical compounds highlights the novelty and applicability of this system, filling a critical gap in literature where reusability studies have rarely addressed real pharmaceutical effluents [74–78].

3.6. Mechanism of ECO-PECO and performance evaluation of Ag/TiO_2 coated electrodes

The enhanced pollutant removal performance observed in the PECO system can be attributed to the generation of ROS, primarily OH• and (O_2^-•), under the combined influence of applied current and UV irradiation. In Ag/TiO_2-TiO_2 and TiO_2-Ag/TiO_2 electrodes, the photogenerated electrons and holes facilitate redox reactions at the electrode surfaces, promoting oxidative degradation of complex organics. In photo-electrocatalytic oxidation processes, photocatalysts interact with pollutants in aqueous environments and disperse throughout the system. It is well known that electrons on the Ag surface directly transfer to pollutant molecules under dark conditions [81]. However, under UV light, the electrons in TiO_2 are excited and transferred from the valence band to the conduction band, forming an electron-hole pair. These photo-generated electron-hole pairs play a critical role in photocatalytic degradation processes [82]. To minimize these recombination losses and ensure efficient electron transfer, doping strategies using noble metals such as Ag are employed [83].

Generally, the excitation of TiO_2 under irradiation (Eq. (7)) leads to the generation of e^-/h^+ pairs that can recombine unless promptly scavenged, thereby reducing overall photocatalytic efficiency [80]. To suppress recombination, oxidants such as atmospheric O_2 can capture conduction band electrons and form O_2^-•, while valence band holes react with water or hydroxide ions to yield OH• (Eqs. (8), (9)) [74].

The primary role of Ag doping is to act as an electron scavenger, capturing electrons on the TiO_2 surface and facilitating their transfer to O_2. Oxygen, acting as an electron acceptor, generates O_2^-•. The holes in the valence band react with water molecules, resulting in the formation of OH•. These radicals serve as the key reactive species in the photocatalytic degradation of active pharmaceutical compounds [84]. Studies in the literature indicate that the photocatalytic mechanism generally follows similar reaction steps. In general, the photocatalysis process begins with the excitation of the TiO_2 surface under a light source (UV, sunlight) [85].

$$TiO_2 + hv \rightarrow e^- + h^+ \quad (7)$$

$$e^- + O_2 \rightarrow O_2^-\bullet \quad (8)$$

$$h^+ + OH^- \rightarrow OH\bullet \quad (9)$$

$$h^+ + e^- \rightarrow heat\ energy \quad (10)$$

In Ag-doped systems, additional reactions occur where Ag^0 traps electrons (Eq. (11)), and subsequently re-oxidizes (Eq. (12)), enabling continuous ROS formation via a redox cycle (Eqs. (12), (13)). Hydroxyl radicals (E^0 = +3.06 V) are particularly significant as they non-selectively oxidize pharmaceuticals, leading to partial or complete mineralization (Eq. (18)) [74].

The Ag-doped TiO_2 photocatalyst transitions in trace amounts to the aqueous phase during the treatment process, where, in the absence of light, electrons on the Ag surface are transferred directly to the pollutant molecules. When a light source is applied, the electrons in the valence band of TiO_2 are excited and transferred to the conduction band, leading to the following reactions: [19]:

$$e^- + Ag \rightarrow Ag^- \quad (11)$$

$$Ag^- + O_2 \rightarrow Ag + O_2^-\bullet \quad (12)$$

$$h^+ + H_2O \rightarrow H^+ + OH\bullet \quad (13)$$

$$O_2^-\bullet + e^- + H^+ \rightarrow H_2O_2 \quad (14)$$

$$H_2O_2 \rightarrow \bullet OH \quad (15)$$

$$O_2 + 2OH^- + 2h^+ \rightarrow O_3 + H_2O \quad (16)$$

$$O_3 + e^- \rightarrow O_3^- \quad (17)$$

$$OH\bullet + organic\ compound \rightarrow CO_2 + H_2O \quad (18)$$

The photo-generated electrons and holes in the valence and conduction bands can move independently on the surface of the photocatalyst. Electrons in the conduction band react with oxygen present in the environment to form superoxide radicals, while the holes in the valence band interact with water molecules, leading to the formation of hydroxyl radicals. These free radicals rapidly react with organic pollutants, breaking them down into smaller, often less harmful compounds. Due to the high oxidation potential of hydroxyl radicals, this process provides a more effective degradation mechanism compared to traditional oxidants [86,87].

Trapping experiments conducted with scavengers such as benzoquinone, EDTA, and isopropyl alcohol have shown that hydroxyl radicals are the dominant oxidative species, as their inhibition most significantly reduces degradation efficiency [80]. Moreover, temperature plays a role in radical generation and reaction rates. While increasing temperature boosts cavitation and radical production, it may also decrease surface adsorption and oxygen solubility, influencing the degradation rate [88].

The results obtained in this study are presented in Fig. 8, and it is evident that they align closely with the oxidation mechanism. The

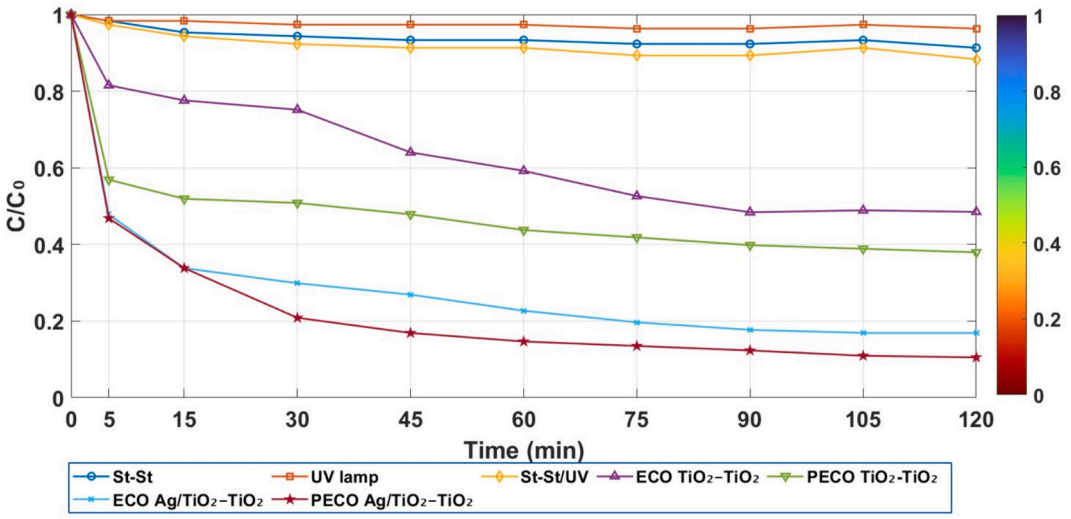


Fig. 8. Variation of normalized concentration (C/C_0) of pharmaceutical industry wastewater over time under different treatment conditions (COD): stainless steel electrode (St-St), UV irradiation only (UV lamp), combined St-St and UV (St-St/UV), electrochemical oxidation (ECO TiO_2-TiO_2), photoelectrochemical oxidation (PECO TiO_2), Ag-doped electrochemical oxidation (ECO Ag/TiO_2-TiO_2), and Ag-doped photoelectrochemical oxidation (PECO Ag/TiO_2-TiO_2) (pH: 5, 0,5 A, 30 °C).

results achieved through photo catalytic oxidation demonstrated higher performance compared to those obtained through electro catalytic oxidation. The comparative analysis of C/C_0 profiles over time across different treatment systems clearly demonstrates the superior degradation efficiency achieved by Ag-doped photoelectrochemical oxidation (PECO Ag/TiO_2-TiO_2). While conventional systems such as UV photolysis (UV lamp) and electrochemical oxidation using TiO_2-coated electrodes (ECO TiO_2-TiO_2) provided moderate reductions in pollutant concentration, the Ag-doped PECO configuration led to the most pronounced decline, reaching a C/C_0 value of 0.1051 within 120 min. This enhanced performance can be attributed to the synergistic effect of Ag doping on the TiO_2 photocatalyst surface, which plays a crucial role in minimizing electron-hole recombination and sustaining ROS generation over time.

Upon UV irradiation, electrons in TiO_2 are excited from the valence band to the conduction band, producing electron-hole (e^-/h^+) pairs (Eq. (7)). In the absence of scavengers, these charge carriers tend to recombine, releasing heat (Eq. (10)) and thus reducing photocatalytic efficiency. Ag nanoparticles, however, act as electron traps (Eq. (11)), facilitating continuous charge separation. The trapped electrons are then transferred to dissolved oxygen, generating superoxide radicals (Eq. (12)), while the photogenerated holes react with water to produce hydroxyl radicals (Eq. (13)). These ROS, particularly OH• with its high oxidation potential, rapidly oxidize pharmaceutical contaminants, leading to effective mineralization.

Compared to the non-doped TiO_2 systems, Ag-doped electrodes maintained lower C/C_0 values throughout the treatment period, indicating sustained ROS activity and reduced recombination rates. The coating strategy applied to the electrodes ensured uniform dispersion of Ag-doped TiO_2 nanoparticles, enhancing active surface area and facilitating interfacial charge transfer. The consistent performance of the PECO Ag/TiO_2-TiO_2 system even at later stages of treatment (e.g., 120 min) underscores the stability and effectiveness of the Ag doping approach in real wastewater matrices, where competitive adsorption and radical scavenging effects typically limit photocatalytic reactions. These results provide compelling evidence that Ag incorporation into TiO_2 electrodes not only improves photo reactivity but also prolongs catalytic activity under combined UV and electrochemical conditions [89,90].

In a similar study conducted by Collivignarelli et al., the COD removal in real pharmaceutical wastewater was limited to 18 % using the photolysis process with UV light alone, while photo electro catalysis using TiO_2 achieved over 40 % removal [91]. This high efficiency can be attributed to the fact that, in the photolysis process, UV light targets only the chromophores, while in the photo electro catalysis process, the hydroxyl radicals generated affect all organic compounds. The results obtained in our study further support the high efficiency of Ag/TiO_2 photocatalysts. The COD removal value of 76.80 % achieved in this study is well above the 40 % level reported in the literature, demonstrating that the addition of Ag significantly improves the photocatalytic performance.

There is a significant body of literature focused on the removal of different pharmaceutical active ingredients. However, studies conducted on real pharmaceutical industry wastewater are quite limited [27]. Photocatalysis processes using Ag/TiO_2 nanoparticles have reported removal efficiencies exceeding 90 % for specific pharmaceutical active ingredients such as Difloxacin hydrochloride, ciprofloxacin, enrofloxacin, danofloxacin [92], Lomefloxacin [62], paracetamol [93]. However, many of these studies have been conducted on model solutions. It is known that organic and inorganic compounds present in real wastewater environments can inhibit photocatalytic reactions [94]. The lower removal efficiencies obtained in our study may be attributed to the synergistic effects of the pollutants due to the complex matrix components present in the real wastewater environment [95]. This could result from competitive adsorption, radical scavenging effects, and binding mechanisms on the photocatalyst surface [96]. These findings emphasize the importance of conducting studies on real wastewater for practical applications and highlight the inadequacy of studies that focus only on specific pollutants.

The efficiency of photocatalytic degradation also depends heavily on pH, which influences the surface charge of TiO_2 and Ag/TiO_2 particles. For example, acidic pH enhances oxidation potential but may limit reaction kinetics due to proton saturation, while alkaline conditions can reduce adsorption due to electrostatic repulsion [97,98]. Since the point of zero charge of Ag-TiO_2 is around 6.6, treatment performance tends to decline in highly basic environments due to increased electrostatic repulsion with anionic pollutants [99].

These findings collectively demonstrate that Ag-doped TiO_2-based photo electrocatalytic systems are highly effective for the treatment of complex pharmaceutical wastewater matrices. The observed COD and UV_{254} removal efficiencies, notably surpassing those reported in similar studies, confirm the synergistic role of Ag as both an electron trap and an ROS promoter. The presence of Ag^+/Ag^0 redox cycling appears to sustain reactive oxygen species formation over time, contributing to

enhanced degradation of both chromophoric and non-chromophoric compounds [74].

Nonetheless, the complexity of real wastewater introduces certain limitations that must be considered. The presence of radical scavengers (e.g., bicarbonates, chlorides), competition for active sites among co-contaminants, and matrix-induced shielding effects may contribute to partial suppression of photocatalytic activity. Moreover, although the process exhibits high oxidative potential, complete mineralization may not always be achieved, as evidenced by the remaining COD and UV_{254} values after treatment. Therefore, coupling photocatalytic systems with complementary treatment methods (e.g., adsorption, biological polishing) could be explored to ensure full compliance with discharge standards.

Importantly, this study provides one of the few experimental evaluations using real pharmaceutical industry wastewater, thus bridging the gap between laboratory-scale contaminant studies and practical field applications. The reproducibility of the process under optimized conditions (pH 5, 0.8 A, 30 min, 30 °C), as well as the demonstrated recyclability of the catalyst further enhances the feasibility of scaling up such systems for continuous-flow treatment scenarios.

Future work should focus on mechanistic elucidation using scavenger experiments, quantification of intermediate byproducts via LC-MS, and long-term stability assessments under dynamic flow conditions. Moreover, understanding how specific wastewater matrix components interact with the catalyst surface could lead to the development of more selective or matrix-resistant materials. Such efforts will be critical in tailoring photocatalytic technologies for robust and energy-efficient treatment of emerging contaminants in real industrial effluents.

3.7. Toxicity removal performance

The acute toxicity of raw and treated wastewater samples was assessed using immobilization-based bioassays across a range of dilution ratios. The findings of this study show that the acute toxicity level of pharmaceutical wastewater is high, with a 97 % immobilization rate observed within 24 h at 100 % concentration in tests conducted on

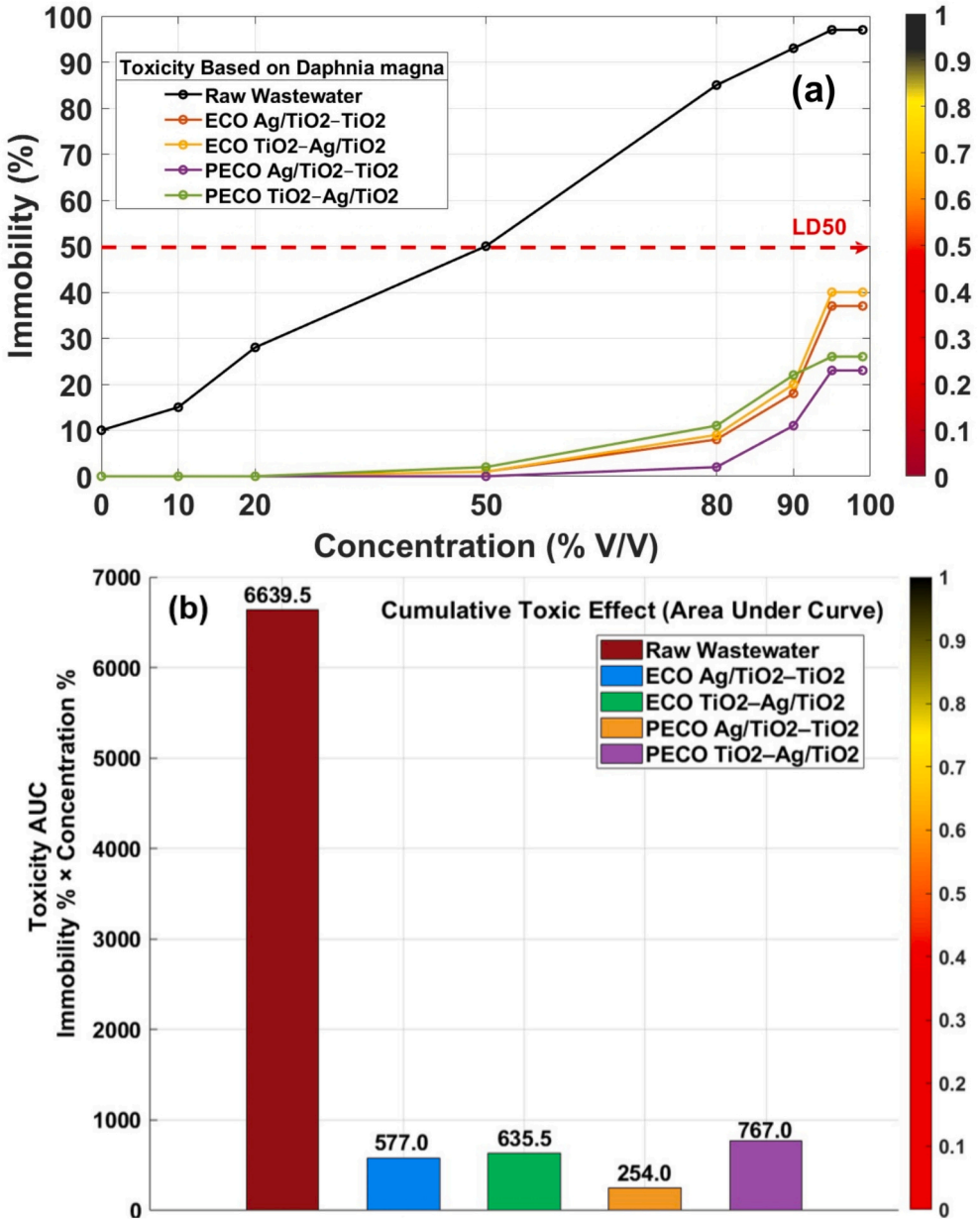


Fig. 9. Toxicity results of raw and treated pharmaceutical industry wastewater a) immobilization, b). Area Under Curve (AUC).

Daphnia magna. These results are consistent with previous studies highlighting the negative impacts of industrial waste containing resistant organic pollutants and bioactive compounds on ecosystems [100,101].

The effectiveness of ECO and PECO in reducing toxicity has been demonstrated, and the results obtained using Ag-doped TiO_2 electrodes further reinforce the efficacy of these processes (Fig. 9). Even in undiluted samples analyzed after treatment, the immobilization rates remained below 50 %, highlighting the potential of advanced oxidation processes (AOPs) to reduce eco-toxicological risks. Both ECO and PECO systems significantly reduced toxicity, but PECO demonstrated superior detoxification potential. The marked reduction in toxicity aligns well with the observed trends in TOC and UV_{254} removal, suggesting that mineralization and aromatic ring cleavage played a critical role in toxicity abatement. In experiments using Ag/TiO_2-TiO_2 electrodes at an 80 % *V*/V wastewater concentration, the immobilization rate dropped to 2 % for PECO and 8 % for ECO. These results indicate that photo electro catalytic processes benefit from synergistic mechanisms that enhance the degradation efficiency of pollutants. This improved performance is largely attributed to the high photocatalytic activity of Ag/TiO_2 under light irradiation, which supports the formation of reactive oxygen species (ROS) and facilitates the breakdown of complex organic pollutants [102].

The role of Ag nanoparticles (NPs) in these systems is critical; their ability to disrupt vital processes such as microbial cell adhesion, DNA replication, and enzymatic activity has been well-documented in antiviral and antibacterial contexts [103]. Furthermore, the integration of Ag NPs with TiO_2 enhances charge separation, prolonging the lifetime of photo-generated electron-hole pairs, which in turn increases the production of reactive oxygen species [104,105].

The study conducted by Pugazhenthiran et al. confirms our findings on the time-dependent detoxification efficacy of Ag/TiO_2 systems, observing a decrease in *A. fischeri* bioluminescence inhibition from 93 % to 37 % after 300 min of photocatalytic treatment [61]. A 1.5-fold increase in degradation rates has been reported for Ti/TiO_2-Ag photoanodes compared to Ti/TiO_2 alone [104]. These results further support the hypothesis that Ag doping enhances photocatalytic efficiency through both electronic and surface interactions.

Despite the progress made, the exact antibacterial mechanisms of Ag/TiO_2 are still not fully elucidated. While the synergy between Ag^+ ions and reactive oxygen species, particularly hydroxyl radicals, has been widely associated [102,106], further studies are needed to clarify the relative contributions of these factors across different microbial taxa and pollutant matrices.

The Area Under Curve (AUC) analysis clearly demonstrates the superior detoxification performance of the applied electrochemical systems (Fig. 9). Raw wastewater exhibited a substantially higher cumulative toxicity, with an AUC value of 6639.5 (Immobility % x Concentration %), confirming its strong ecotoxic potential. In contrast, all treated samples showed a dramatic reduction in total toxic impact. Among them, the PECO Ag/TiO_2-TiO_2 configuration yielded the lowest AUC (254.0), followed by PECO TiO_2-Ag/TiO_2 and ECO variants. These results confirm the enhanced ability of PECO to mitigate both acute toxicity and bioavailable toxic intermediates. The AUC-based comparison offers a robust and integrative metric for evaluating the environmental safety of treated effluents.

As a result of this study demonstrates that Ag/TiO_2-based photoelectrochemical processes, especially PECO, present a promising strategy for detoxifying pharmaceutical wastewater. The technology's high antimicrobial efficacy, balanced with reduced ecotoxicity, positions it as a viable candidate for sustainable wastewater treatment. Future research should prioritize optimizing Ag/TiO_2 loading to maximize degradation efficiency while minimizing environmental impacts. Long-term studies assessing the fate of Ag nanoparticles and their interactions with aquatic ecosystems will be crucial to ensuring the scalability and sustainability of this approach.

4. Future perspectives

This study highlights the strong potential of Ag-doped TiO_2-based photo electrocatalytic systems for the treatment of real pharmaceutical industry wastewater. The combined use of photocatalysis and electrochemical oxidation in a reagent-free configuration offers several advantages, including enhanced removal efficiencies due to synergistic radical generation, operational simplicity under mild conditions (pH 5, 0.8 A, 30 °C), and partial energy recovery through hydrogen production. Additionally, the photocatalyst demonstrated notable recyclability over multiple cycles, supporting its potential for long-term and semi-continuous applications. Despite these promising outcomes, certain limitations remain. The complex nature of pharmaceutical effluents, which often contain a diverse range of organic and inorganic constituents, may reduce treatment efficiency due to radical scavenging, surface fouling, and competitive adsorption. Although high levels of COD and UV_{254} removal were achieved, complete mineralization was not always observed, indicating the possible accumulation of intermediate degradation products. Moreover, repeated use of the Ag-doped catalyst may lead to minor Ag^+ leaching, which could pose environmental and stability concerns over extended operation. To address these challenges and advance the practical implementation of this technology, future research should focus on clarifying the degradation mechanism through radical scavenger experiments and intermediate by-product analysis, evaluating catalyst durability and leaching behavior under continuous-flow conditions, and integrating polishing steps such as biological or membrane treatments to achieve complete mineralization. Furthermore, development of more selective, matrix-resistant photocatalysts and comprehensive techno-economic assessments, including hydrogen utilization strategies, will be essential for scaling up to industrial applications. Overall, while the system presents a robust platform for sustainable wastewater treatment, further optimization in both catalyst design and process configuration is necessary for real-world deployment.

5. Conclusion

This study comprehensively evaluated the efficiency of PECO for the treatment of pharmaceutical wastewater, focusing on process optimization, pollutant removal performance, and ecotoxicological effects. Optimization studies based on Central Composite Design (CCD) revealed the significant influence of pH, reaction time, current density, and temperature on COD and UV_{254} removal efficiencies. Validation tests confirmed that the developed model could predict removal efficiencies with 98 % accuracy, demonstrating the robustness of the optimization approach. The highest COD removal efficiency of 76 % was achieved under optimized PECO conditions.

Beyond pollutant removal, the ecotoxicity assessment provided a holistic perspective, addressing the synergistic toxic effects of pharmaceutical compounds that are often overlooked in conventional studies. Acute toxicity tests using *Daphnia magna* indicated a significant reduction in immobilization from 97 % in untreated wastewater to 23 % after PECO treatment. This improvement is attributed to the enhanced charge separation and increased reactive oxygen species (ROS) generation facilitated by Ag/TiO_2 electrodes, which not only promoted the degradation of organic pollutants but also mitigated toxic by-product formation.

Overall, the findings of this study highlight PECO as a promising technology for pharmaceutical wastewater treatment due to its high removal efficiency, low energy consumption, and strong detoxification capability. Future research should focus on improving energy efficiency, ensuring scalability, and gaining deeper insights into the environmental implications of nanoparticles to advance the practical applicability of this technology.

CRediT authorship contribution statement

Ayse Elif Ates: Writing – original draft, Software, Methodology. **Sinan Ates:** Writing – original draft, Investigation. **Serdar Aydın:** Supervision, Methodology. **Gamze Varank:** Writing – review & editing, Supervision.

Declaration of competing interest

The authors declare that they have no known competing financial interests or personal relationships that could have appeared to influence the work reported in this paper.

Acknowledgments

This article is derived from the doctoral thesis entitled *"Treatment of industrial wastewater containing highly resistant organic compounds with combined catalytic oxidation"*, conducted at the Department of Environmental Engineering, Istanbul University-Cerrahpaşa. The authors gratefully acknowledge the support of the institution during the execution of this research.

Artificial intelligence-based tools were utilized to enhance the clarity, coherence, and readability of the manuscript.

This study was funded by Scientific Research Projects Coordination Unit of Istanbul University-Cerrahpasa. Project number: FDK-2023-37294.

Appendix A. Supplementary data

Supplementary data to this article can be found online at https://doi.org/10.1016/j.jwpe.2025.108109.

Data availability

Data will be made available on request.

References

[1] A. Shah, M. Shah, Characterisation and bioremediation of wastewater: a review exploring bioremediation as a sustainable technique for pharmaceutical wastewater, Groundw. Sustain. Dev. 11 (2020) 100383.
[2] J. Xue, D. Lei, X. Zhao, Y. Hu, S. Yao, K. Lin, Z. Wang, C. Cui, Antibiotic residue and toxicity assessment of wastewater during the pharmaceutical production processes, Chemosphere 291 (2022) 132837.
[3] E. Strade, D. Kalnina, Cost effective method for toxicity screening of pharmaceutical wastewater containing inorganic salts and harmful organic compounds, Environ. Clim. Technol. 23 (2019) 52–63.
[4] Y. Li, C. Li, Z. Wang, Y. Liu, Y. Jia, F. Li, R. Ren, A. Ikhlaq, J. Kumirska, E. M. Siedlecka, Navigating the complexity of pharmaceutical wastewater treatment by "effective strategy, emerging technology, and sustainable solution,", J. Water Process Eng. 63 (2024) 105404.
[5] S.N. Kumar, P.L. Muralidhara, L. Hiremath, P.R. Swathi, A recent advancement on treatment Technologies For Handling of pharma waste water, Res. J. Pharm. Technol. 13 (2020) 1981–1986.
[6] M.A. Oturan, J.-J. Aaron, Advanced oxidation processes in water/wastewater treatment: principles and applications. A review, Crit. Rev. Environ. Sci. Technol. 44 (2014) 2577–2641.
[7] S.N. Ahmed, W. Haider, Heterogeneous photocatalysis and its potential applications in water and wastewater treatment: a review, Nanotechnology 29 (2018) 342001.
[8] J. Qiao, Y. Xiong, Electrochemical oxidation technology: a review of its application in high-efficiency treatment of wastewater containing persistent organic pollutants, J. Water Process Eng. 44 (2021) 102308.
[9] C.A. Martínez-Huitle, E. Brillas, Decontamination of wastewaters containing synthetic organic dyes by electrochemical methods: a general review, Appl Catal B 87 (2009) 105–145.
[10] A. Taqieddin, S. Sarrouf, M.F. Ehsan, A.N. Alshawabkeh, New insights on designing the next-generation materials for electrochemical synthesis of reactive oxidative species towards efficient and scalable water treatment: a review and perspectives, J. Environ. Chem. Eng. 11 (2023) 111384.
[11] M. Sayed, C. Zhao, E. Mousset, J.A. Khan, D.D. Dionysiou, Decomposition of refractory organics in wastewater by electrocatalytic reduction: mechanism, challenges, and future perspectives, Curr. Opin. Chem. Eng. 44 (2024) 101016.
[12] D.S.M. Constantino, M.M. Dias, A.M.T. Silva, J.L. Faria, C.G. Silva, Intensification strategies for improving the performance of photocatalytic processes: a review, J. Clean. Prod. 340 (2022) 130800.
[13] H. Liu, C. Wang, G. Wang, Photocatalytic advanced oxidation processes for water treatment: recent advances and perspective, Chemistry–An Asian Journal 15 (2020) 3239–3253.
[14] A. Anglada, A. Urtiaga, I. Ortiz, Contributions of electrochemical oxidation to waste-water treatment: fundamentals and review of applications, J. Chem. Technol. Biotechnol. 84 (2009) 1747–1755.
[15] S.O. Ganiyu, C.A. Martínez-Huitle, M.A. Oturan, Electrochemical advanced oxidation processes for wastewater treatment: advances in formation and detection of reactive species and mechanisms, Curr. Opin. Electrochem. 27 (2021) 100678.
[16] Y. Sari, P.L. Gareso, B. Armynah, D. Tahir, A review of TiO2 photocatalyst for organic degradation and sustainable hydrogen energy production, Int. J. Hydrogen Energy 55 (2024) 984–996.
[17] H. Khan, M.U.H. Shah, Modification strategies of TiO2 based photocatalysts for enhanced visible light activity and energy storage ability: a review, J. Environ. Chem. Eng. 11 (2023) 111532.
[18] D.A.K. Ramadhani, N. Sholeha, N.N. Khusna, M. Diantoro, A.N. Afandi, Z. Osman, H. Pujiarti, Ag-doped TiO2 as photoanode for high performance dye sensitized solar cells, Mater. Sci. Energy Technol. 7 (2024) 274–281.
[19] D. Kanakaraju, F.D. anak Kutiang, Y.C. Lim, P.S. Goh, Recent progress of ag/TiO2 photocatalyst for wastewater treatment: doping, co-doping, and green materials functionalization, Appl. Mater. Today 27 (101500) (2022).
[20] M.N. Chong, B. Jin, C.W.K. Chow, C. Saint, Recent developments in photocatalytic water treatment technology: a review, Water Res. 44 (2010) 2997–3027.
[21] N. Ahmadpour, M. Nowrouzi, V.M. Avargani, M.H. Sayadi, S. Zendehboudi, Design and optimization of TiO2-based photocatalysts for efficient removal of pharmaceutical pollutants in water: recent developments and challenges, J. Water Process Eng. 57 (2024) 104597.
[22] W.J. Tseng, Y.-C. Chuang, Y.-A. Chen, Mesoporous Fe3O4@ Ag@ TiO2 nanocomposite particles for magnetically recyclable photocatalysis and bactericide, Adv. Powder Technol. 29 (2018) 664–671.
[23] C.A. Aguilar, C. Montalvo, B.B. Zermeño, R.M. Cerón, J.G. Cerón, F. Anguebes, M. A. Ramírez, Photocatalytic degradation of acetaminophen, tergitol and nonylphenol with catalysts TiO 2/Ag under UV and Vis light, Int. J. Environ. Sci. Technol. 16 (2019) 843–852.
[24] M. Motamedi, L. Yerushalmi, F. Haghighat, Z. Chen, Recent developments in photocatalysis of industrial effluents: a review and example of phenolic compounds degradation, Chemosphere 296 (2022) 133688.
[25] R.H. Myers, D.C. Montgomery, C.M. Anderson-Cook, Response surface methodology: process and product optimization using designed experiments, John Wiley & Sons, 2016.
[26] D.C. Montgomery, Design and analysis of experiments, John Wiley & Sons, 2017.
[27] S. Wu, Y.H. Hu, A comprehensive review on catalysts for electrocatalytic and photoelectrocatalytic degradation of antibiotics, Chem. Eng. J. 409 (2021) 127739.
[28] E.W. Rice, R.B. Baird, A.D. Eaton, L.S. Clesceri, Standard methods for the examination of water and wastewater, 2012.
[29] T. Yuranova, R. Mosteo, J. Bandara, D. Laub, J. Kiwi, Self-cleaning cotton textiles surfaces modified by photoactive SiO2/TiO2 coating, J. Mol. Catal. A Chem. 244 (2006) 160–167.
[30] M.M. Abutalib, A. Rajeh, Enhanced structural, electrical, mechanical properties and antibacterial activity of Cs/PEO doped mixed nanoparticles (Ag/TiO2) for food packaging applications, Polym. Test. 93 (2021) 107013, https://doi.org/10.1016/J.POLYMERTESTING.2020.107013.
[31] M.I. Din, R. Khalid, Photocatalysis of pharmaceuticals and organic dyes in the presence of silver-doped TiO2 photocatalyst–a critical review, Int. J. Environ. Anal. Chem. 105 (2025) 276–300, https://doi.org/10.1080/03067319.2023.2258795.
[32] H. Chakhtouna, H. Benzeid, N. Zari, A. El Kacem Qaiss, R. Bouhfid, Recent progress on Ag/TiO2 photocatalysts: photocatalytic and bactericidal behaviors, Environmental Science and Pollution Research (2021) 44638–44666, https://doi.org/10.1007/S11356-021-14996-Y, 2021 28:33 28.
[33] S. Shukla, H. Pandey, P. Singh, A.K. Tiwari, V. Baranwal, A.C. Pandey, Synergistic impact of photocatalyst and dopants on pharmaceutical-polluted waste water treatment: a review, Environmental Pollutants and Bioavailability 33 (2021) 347–364, https://doi.org/10.1080/26395940.2021.1987843.
[34] M. Antonopoulou, Homogeneous and heterogeneous photocatalysis for the treatment of pharmaceutical industry wastewaters: a review, Toxics 10 (9) (2022) 539, https://doi.org/10.3390/TOXICS10090539.
[35] K. Jiang, M. Kusdianto, A. Kubo, G. Chen, W. Hu, J. Yu, E. Nyankson, N. Yeboah, S. Ocrah Jnr., S. Onaja, T. Mensah, J.K. Efavi, The effect of synthesis route on the photocatalytic performance of Ag-TiO2 using rhodamine b dyes, pesticides, and pharmaceutical waste as model pollutants, Mater. Res. Express 9 (2022) 094001, https://doi.org/10.1088/2053-1591/AC871F.
[36] M.I. Badawy, E.M.R. Souaya, T.A. Gad-Allah, M.S. Abdel-Wahed, M. Ulbricht, Fabrication of Ag/TiO2 photocatalyst for the treatment of simulated hospital wastewater under sunlight, Environ. Prog. Sustain. Energy 33 (2014) 886–894, https://doi.org/10.1002/EP.11869;REQUESTEDJOURNAL:JOURNAL:19447450;WEBSITE:WEBSITE:AICHE;JOURNAL:JOURNAL:15475921;WGROUP:STRING:PUBLICATION.
[37] D. Kanakaraju, F.D. anak Kutiang, Y.C. Lim, P.S. Goh, Recent progress of ag/TiO2 photocatalyst for wastewater treatment: doping, co-doping, and green materials

functionalization, Appl. Mater. Today 27 (2022) 101500, https://doi.org/10.1016/J.APMT.2022.101500.
[38] L.M. Santos, W.A. Machado, M.D. França, K.A. Borges, R.M. Paniago, A.O. T. Patrocinio, A.E.H. Machado, Structural characterization of Ag-doped TiO2 with enhanced photocatalytic activity, RSC Adv. 5 (2015) 103752–103759, https://doi.org/10.1039/C5RA22647C.
[39] O. Oecd, Guideline for testing of chemicals. *Daphnia* sp., acute immobilisation test, 2004.
[40] J.L. Weishaar, G.R. Aiken, B.A. Bergamaschi, M.S. Fram, R. Fujii, K. Mopper, Evaluation of specific ultraviolet absorbance as an indicator of the chemical composition and reactivity of dissolved organic carbon, Environ. Sci. Technol. 37 (2003) 4702–4708.
[41] H. Huang, C.W.K. Chow, B. Jin, Characterisation of dissolved organic matter in stormwater using high-performance size exclusion chromatography, J. Environ. Sci. 42 (2016) 236–245.
[42] J. Li, G. Luo, L. He, J. Xu, J. Lyu, Analytical approaches for determining chemical oxygen demand in water bodies: a review, Crit. Rev. Anal. Chem. 48 (2018) 47–65.
[43] M. Eddy, M. Abu-Orf, G. Bowden, F.L. Burton, W. Pfrang, H.D. Stensel, G. Tchobanoglous, R. Tsuchihashi, A. (Firm), Wastewater engineering: treatment and resource recovery, McGraw Hill Education, 2014.
[44] E. Can-Güven, S.Y. Guvenc, N. Kavan, G. Varank, Paper mill wastewater treatment by Fe2+ and heat-activated persulfate oxidation: process modeling and optimization, Environ. Prog. Sustain. Energy 40 (2021) e13508.
[45] G. Varank, S. Yazici Guvenc, A. Demir, A comparative study of electrocoagulation and electro-Fenton for food industry wastewater treatment: multiple response optimization and cost analysis, Sep. Sci. Technol. 53 (2018) 2727–2740.
[46] R. Shokoohi, R. Najafi-Vosough, A. Shabanloo, Z. Torkshavand, M.M. Mahmoudi, M. Attar Abasi, Removing heavy metals and improving the dewaterability of sewage sludge with the bioleaching process by Thiobacillus Ferrooxidans bacteria, Appl Water Sci 15 (2025) 34.
[47] Q. Zhang, J. Peng, H. Xiong, S. Jiang, W. Li, X. Fu, S. Shang, J. Xu, G. He, Cold plasma-activated Ni-Co tandem catalysts with CN vacancies for enhancing CH4 electrocatalytic to methyl formate, Applied Catalysis B: Environment and Energy 362 (2025) 124759.
[48] A.R. Rahmani, A. Shabanloo, M. Fazlzadeh, Y. Poureshgh, M. Vanaeitabar, Optimization of sonochemical decomposition of ciprofloxacin antibiotic in US/PS/nZVI process by CCD-RSM method, Desalin. Water Treat. 145 (2019) 300–308.
[49] L.-C. Zhao, J. Liang, W. Li, K.-M. Cheng, X. Xia, X. Deng, G.-L. Yang, The use of response surface methodology to optimize the ultrasound-assisted extraction of five anthraquinones from Rheum palmatum L, Molecules 16 (2011) 5928–5937.
[50] L.-C. Zhao, Y. He, X. Deng, X.-H. Xia, J. Liang, G.-L. Yang, W. Li, H. Wang, Ultrasound-assisted extraction of syringin from the bark of Ilex rotunda thumb using response surface methodology, Int. J. Mol. Sci. 13 (2012) 7607–7616.
[51] L.-C. Zhao, Y. He, X. Deng, G.-L. Yang, W. Li, J. Liang, Q.-L. Tang, Response surface modeling and optimization of accelerated solvent extraction of four lignans from fructus schisandrae, Molecules 17 (2012) 3618–3629.
[52] D.C. Montgomery, G.C. Runger, Applied statistics and probability for engineers, John Wiley & Sons, 2010.
[53] Y.W. Nam, Hyers-ulam stability of elliptic Möbius difference equation, Cogent Math. Stat. 5 (2018) 1492338.
[54] S. Ates, A. Anwar, A.E. Ates, B. Yuzer, Y. Bicer, Nutrient recovery and hydrogen production from wastewater by electrodialysis process: optimization using response surface methodology, J. Water Process Eng. 71 (2025) 107390.
[55] Z.T. Alismaeel, A.H. Abbar, O.F. Saeed, Application of central composite design approach for optimisation of zinc removal from aqueous solution using a flow-by fixed bed bioelectrochemical reactor, Sep. Purif. Technol. 287 (2022) 120510.
[56] S. Daryazadeh, M. Yavari, S.-R. Madani, A. Taghavi-Ardakani, M.J. Azadchahr, F. Shayeghi, Correlation between the e-learning attitude and academic achievement of medical students in clinical levels, Educational Research in Medical Sciences 10 (2021).
[57] J. Jaafari, H. Barzanouni, S. Mazloomi, N.A.A. Farahani, K. Sharafi, P. Soleimani, G.A. Haghighat, Effective adsorptive removal of reactive dyes by magnetic chitosan nanoparticles: kinetic, isothermal studies and response surface methodology, Int. J. Biol. Macromol. 164 (2020) 344–355.
[58] M.A. Ahmad, R. Alrozi, Optimization of preparation conditions for mangosteen peel-based activated carbons for the removal of Remazol Brilliant Blue R using response surface methodology, Chem. Eng. J. 165 (2010) 883–890.
[59] A. Ashrafi, B. Tessem, K. Enberg, in: Swedish Artificial Intelligence Society (Ed.), Analysing unlabeled data with randomness and noise: the case of fishery catch reports, 2024, pp. 204–212.
[60] A.E. ATEŞ, S. BEKTAŞ, Ş. ZENGİN, A. Yaren, A. Sinan, H. SELÇUK, Integrated salt and energy recovery from dyeing wastewater via Fenton and photo-Fenton oxidation: industrial approach, J. Environ. Chem. Eng. (2025) 115930.
[61] N. Pugazhenthiran, S. Murugesan, H. Valdés, M. Selvaraj, P. Sathishkumar, P. G. Smirniotis, S. Anandan, R.V. Mangalaraja, Photocatalytic oxidation of ceftiofur sodium under UV–visible irradiation using plasmonic porous Ag-TiO2 nanospheres, J. Ind. Eng. Chem. 105 (2022) 384–392.
[62] R.M. Kulkarni, R.S. Malladi, M.S. Hanagadakar, M.R. Doddamani, U.K. Bhat, Ag-TiO2 nanoparticles for photocatalytic degradation of lomefloxacin, Desalin. Water Treat. 57 (2016) 16111–16118.
[63] A.C.F.P. Fuhr, C.F. de Azevedo, N. Ahmad, S. Mohandoss, G.L. Dotto, F. M. Machado, Exploring diclofenac potassium adsorption on activated carbon: a comprehensive statistical physics and experimental approach, J. Mol. Liq. 407 (2024) 125191.
[64] N. Galvão, J.B. de Souza, C.M. de Sousa Vidal, Landfill leachate treatment by electrocoagulation: effects of current density and electrolysis time, J. Environ. Chem. Eng. 8 (2020) 104368.
[65] F.L. Souza, C. Sáez, P. Cañizares, M.A. Rodrigo, Improving photolytic treatments with electrochemical technology, Sep. Purif. Technol. 235 (2020) 116229.
[66] F. Cai, S. Cai, Z. Tu, Proton exchange membrane fuel cell (PEMFC) operation in high current density (HCD): problem, progress and perspective, Energ. Conver. Manage. 307 (2024) 118348.
[67] B.B. Garcia, G. Lourinho, P. Romano, P.S.D. Brito, Photocatalytic degradation of swine wastewater on aqueous TiO2 suspensions: optimization and modeling via Box-Behnken design, Heliyon 6 (2020).
[68] V.M. Avargani, S. Zendehboudi, S. Osfouri, A. Rostami, Performance evaluation of a solar nano-photocatalytic reactor for wastewater treatment applications: reaction kinetics, CFD, and scale-up perspectives, J. Clean. Prod. 421 (2023) 138240.
[69] H.A. Maitlo, Z. Hu, I. Ali, G. Maitlo, D.-H. Lim, M.N. Afridi, M. Zhou, Recent development in advanced photocatalytic materials for oxidative removal of bisphenol, J. Clean. Prod. 434 (2024) 140291.
[70] F.L. Guzmán-Duque, R.E. Palma-Goyes, I. González, G. Peñuela, R.A. Torres-Palma, Relationship between anode material, supporting electrolyte and current density during electrochemical degradation of organic compounds in water, J. Hazard. Mater. 278 (2014) 221–226.
[71] T. Li, Y. Jiang, X. An, H. Liu, C. Hu, J. Qu, Transformation of humic acid and halogenated byproduct formation in UV-chlorine processes, Water Res. 102 (2016) 421–427.
[72] S. Lu, G. Zhang, Recent advances on inactivation of waterborne pathogenic microorganisms by (photo) electrochemical oxidation processes: design and application strategies, J. Hazard. Mater. 431 (2022) 128619.
[73] E. Öztürk, A.E. Ateş, H. Selçuk, S. Ateş, Treatment of real pharmaceutical industry wastewater by photo-Fenton oxidation using the response surface methodology, evaluation of diclofenac degradation and toxicity, Engineering Science and Technology, an International Journal 64 (2025) 102004.
[74] M.I. Din, R. Khalid, Photocatalysis of pharmaceuticals and organic dyes in the presence of silver-doped TiO2 photocatalyst–a critical review, Int. J. Environ. Anal. Chem. 105 (2025) 276–300.
[75] K. Aghasian, A. Moridi, A. Mirbagheri, M. Abbaspour, A conflict resolution method for waste load reallocation in river systems, Int. J. Environ. Sci. Technol. 16 (2019) 79–88.
[76] S.S. Boxi, S. Paria, Visible light induced enhanced photocatalytic degradation of organic pollutants in aqueous media using Ag doped hollow TiO 2 nanospheres, RSC Adv. 5 (2015) 37657–37668.
[77] A.K. Gupta, A. Pal, C. Sahoo, Photocatalytic degradation of a mixture of Crystal Violet (Basic Violet 3) and Methyl Red dye in aqueous suspensions using Ag+ doped TiO2, Dyes Pigments 69 (2006) 224–232.
[78] C. Sahoo, A.K. Gupta, I.M. Sasidharan Pillai, Photocatalytic degradation of methylene blue dye from aqueous solution using silver ion-doped TiO2 and its application to the degradation of real textile wastewater, J. Environ. Sci. Health A 47 (2012) 1428–1438.
[79] H. Chaker, L. Chérif-Aouali, S. Khaoulani, A. Bengueddach, S. Fourmentin, Photocatalytic degradation of methyl orange and real wastewater by silver doped mesoporous TiO2 catalysts, J. Photochem. Photobiol. A Chem. 318 (2016) 142–149.
[80] T. Ali, A. Ahmed, U. Alam, I. Uddin, P. Tripathi, M. Muneer, Enhanced photocatalytic and antibacterial activities of Ag-doped TiO2 nanoparticles under visible light, Mater. Chem. Phys. 212 (2018) 325–335.
[81] E. Brillas, S. Garcia-Segura, Recent progress of applied TiO2 photoelectrocatalysis for the degradation of organic pollutants in wastewaters, J. Environ. Chem. Eng. 11 (2023) 109635.
[82] M.A.U. Olea, J. de J.P. Bueno, A.X.M. Pérez, Nanometric and surface properties of semiconductors correlated to photocatalysis and photoelectrocatalysis applied to organic pollutants–a review, J. Environ. Chem. Eng. 9 (2021) 106480.
[83] D. Gogoi, A. Namdeo, A.K. Golder, N.R. Peela, Ag-doped TiO2 photocatalysts with effective charge transfer for highly efficient hydrogen production through water splitting, Int. J. Hydrogen Energy 45 (2020) 2729–2744.
[84] D. Kanakaraju, B.D. Glass, M. Oelgemöller, Advanced oxidation process-mediated removal of pharmaceuticals from water: a review, J. Environ. Manage. 219 (2018) 189–207.
[85] R. Mohammadi, W. Tang, M. Sillanpää, A systematic review and statistical analysis of nutrient recovery from municipal wastewater by electrodialysis, Desalination 498 (2021) 114626.
[86] C. Karthikeyan, P. Arunachalam, K. Ramachandran, A.M. Al-Mayouf, S. Karuppuchamy, Recent advances in semiconductor metal oxides with enhanced methods for solar photocatalytic applications, J. Alloys Compd. 828 (2020) 154281.
[87] D. Zhu, Q. Zhou, Action and mechanism of semiconductor photocatalysis on degradation of organic pollutants in water treatment: a review, Environ Nanotechnol Monit Manag 12 (2019) 100255.
[88] Z.L. Wang, Oxide nanobelts and nanowires—growth, properties and applications, J. Nanosci. Nanotechnol. 8 (2008) 27–55.
[89] J. Wang, S. Wang, Reactive species in advanced oxidation processes: formation, identification and reaction mechanism, Chem. Eng. J. 401 (2020) 126158.
[90] N. Zhang, E.P. Tsang, J. Chen, Z. Fang, D. Zhao, Critical role of oxygen vacancies in heterogeneous Fenton oxidation over ceria-based catalysts, J. Colloid Interface Sci. 558 (2020) 163–172.
[91] M.C. Collivignarelli, A. Abbà, M.C. Miino, H. Arab, M. Bestetti, S. Franz, Decolorization and biodegradability of a real pharmaceutical wastewater treated

by H2O2-assisted photoelectrocatalysis on TiO2 meshes, J. Hazard. Mater. 387 (2020) 121668.
[92] M.I. Din, R. Khalid, Photocatalysis of pharmaceuticals and organic dyes in the presence of silver-doped TiO2 photocatalyst–a critical review, Int. J. Environ. Anal. Chem. 105 (2025) 276–300.
[93] Y. Cherif, H. Azzi, K. Sridharan, S. Ji, H. Choi, M.G. Allan, S. Benaissa, K. Saidi-Bendahou, L. Damptey, C.S. Ribeiro, Facile synthesis of gram-scale mesoporous Ag/TiO2 photocatalysts for pharmaceutical water pollutant removal and green hydrogen generation, ACS Omega 8 (2022) 1249–1261.
[94] T. Ahuja, U. Brighu, K. Saxena, Recent advances in photocatalytic materials and their applications for treatment of wastewater: a review, J. Water Process Eng. 53 (2023) 103759.
[95] J.J. Rueda-Márquez, C. Palacios-Villarreal, M. Manzano, E. Blanco, M.R. del Solar, I. Levchuk, Photocatalytic degradation of pharmaceutically active compounds (PhACs) in urban wastewater treatment plants effluents under controlled and natural solar irradiation using immobilized TiO2, Sol. Energy 208 (2020) 480–492.
[96] S. Natarajan, H.C. Bajaj, R.J. Tayade, Recent advances based on the synergetic effect of adsorption for removal of dyes from waste water using photocatalytic process, J. Environ. Sci. 65 (2018) 201–222.
[97] M.B. Suwarnkar, R.S. Dhabbe, A.N. Kadam, K.M. Garadkar, Enhanced photocatalytic activity of Ag doped TiO2 nanoparticles synthesized by a microwave assisted method, Ceram. Int. 40 (2014) 5489–5496.
[98] M.I. Badawy, E.M.R. Souaya, T.A. Gad-Allah, M.S. Abdel-Wahed, M. Ulbricht, Fabrication of Ag/TiO2 photocatalyst for the treatment of simulated hospital wastewater under sunlight, Environ. Prog. Sustain. Energy 33 (2014) 886–894.
[99] W. Bahnemann, M. Muneer, M.M. Haque, Titanium dioxide-mediated photocatalysed degradation of few selected organic pollutants in aqueous suspensions, Catal. Today 124 (2007) 133–148.
[100] A.B. Djurišić, Y. He, A. Ng, Visible-light photocatalysts: prospects and challenges, APL Mater. 8 (2020).
[101] J.Z.X. Heng, K.Y. Tang, M.D. Regulacio, M. Lin, X.J. Loh, Z. Li, E. Ye, Solar-powered photodegradation of pollutant dyes using silver-embedded porous TiO2 nanofibers, Nanomaterials 11 (2021) 856.
[102] J. Ma, Z. Xiong, T.D. Waite, W.J. Ng, X.S. Zhao, Enhanced inactivation of bacteria with silver-modified mesoporous TiO2 under weak ultraviolet irradiation, Microporous Mesoporous Mater. 144 (2011) 97–104.
[103] M. Sharma, A. Yadav, M.K. Mandal, K.K. Dubey, TiO2 based photocatalysis: a valuable approach for the removal of pharmaceuticals from aquatic environment, Int. J. Environ. Sci. Technol. 20 (2023) 4569–4584.
[104] M.F. Brugnera, M. Miyata, G.J. Zocolo, C.Q.F. Leite, M.V.B. Zanoni, A photoelectrocatalytic process that disinfects water contaminated with mycobacterium kansasii and Mycobacterium avium, Water Res. 47 (2013) 6596–6605.
[105] M.F. Haris, A.M. Didit, M. Ibadurrohman, Silver doped TiO2 photocatalyst for disinfection of *E. coli* and microplastic pollutant degradation in water, Asian J. Chem. 33 (2021) 2038–2042.
[106] A.E. Ateş, A.T.E.Ş. Sinan, B. Yüzer, H. Selçuk, A Holistic Approach to Treating Industrial Effluents: Photo-Electro-Assisted Fenton-Like Strategy for Effective Degradation and Detoxification, J. Clean. Prod. 145575 (2025).